

Non-Destructive Structural Strength Monitoring using Micro- Electro Mechanical Systems (MEMS)



Author

MUHAMMAD HAMID ALI

2011-NUST-MsPhD-Mts-19

Supervisor

Dr. UMER IZHAR

DEPARTMENT OF MECHATRONICS ENGINEERING
COLLEGE OF ELECTRICAL & MECHANICAL ENGINEERING
NATIONAL UNIVERSITY OF SCIENCES AND TECHNOLOGY
ISLAMABAD
AUGUST, 2015

Non-Destructive Structural Strength Monitoring using Micro-
Electro Mechanical Systems (MEMS)

Author

MUHAMMAD HAMID ALI

2011-NUST-Ms PhD-Mts-19

A thesis submitted in partial fulfillment of the requirements for the degree of
MS Mechatronics Engineering

Thesis Supervisor:

Dr.UMER IZHAR

Thesis Supervisor's Signature: _____

DEPARTMENT OF MECHATRONICS ENGINEERING
COLLEGE OF ELECTRICAL & MECHANICAL ENGINEERING
NATIONAL UNIVERSITY OF SCIENCES AND TECHNOLOGY,

ISLAMABAD

AUGUST, 2015

Declaration

I certify that this research work titled “*Non-Destructive Structural Strength Monitoring using Micro-Electro Mechanical Systems (MEMS)*” is my own work. The work has not been presented elsewhere for assessment. The material that has been used from other sources it has been properly acknowledged / referred.

Signature of Student

Muhammad Hamid Ali

2011-NUST-Ms PhD-Mts-19

Language Correctness Certificate

This thesis has been read by an English expert and is free of typing, syntax, semantic, grammatical and spelling mistakes. Thesis is also according to the format given by the university.

Signature of Student

Muhammad Hamid Ali

2011-NUST-Ms PhD-Mts-19

Signature of Supervisor

Copyright Statement

- Copyright in text of this thesis rests with the student author. Copies (by any process) either in full, or of extracts, may be made only in accordance with instructions given by the author and lodged in the Library of NUST College of E&ME. Details may be obtained by the Librarian. This page must form part of any such copies made. Further copies (by any process) may not be made without the permission (in writing) of the author.
- The ownership of any intellectual property rights which may be described in this thesis is vested in NUST College of E&ME, subject to any prior agreement to the contrary, and may not be made available for use by third parties without the written permission of the College of E&ME, which will prescribe the terms and conditions of any such agreement.
- Further information on the conditions under which disclosures and exploitation may take place is available from the Library of NUST College of E&ME, Rawalpindi.

Acknowledgements

First of all Thanks to ALLAH ALMIGHTY, the alone creator of the worlds and universe, who is the most beneficent and the most merciful, Indeed all praise to ALLAH the alone and one. I am thankful to my beloved parents who raised me when I was not capable of walking and continued to support me throughout in every department of my life.

I would also like to express special thanks to my supervisor Dr. Umer Izhar for his help throughout my thesis, he is always a source of inspiration for me. I would also like to thank my supervisor for his cooperation and support throughout the thesis phase, his guidance, approach, availability, time sparing and whatever was possible on his behalf, whenever and wherever required and most importantly his patience, calmness and motivating attitude in the whole thesis process.

I would also like to pay my regards to GEC members Dr. Faraz Ahmed Khan, Dr. Adnan Masood and Dr. Umar Shahbaz for their support and cooperation. I would also like to thank Dr. Mubashir for his guidance and valuable advices. I would also like to thank Lec Usman Asad for his wonderful guidance, help and unconditional support.

Finally, I would like to express my gratitude to all the individuals who have rendered valuable assistance during the entire tenure.

Dedicated to my exceptional parents especially my mother, adored siblings and my some very special friends whose tremendous support and cooperation led me to this wonderful accomplishment

Abstract

Damage and Vibrations are a local phenomenon that appears in the structure (concrete/mechanical) and needs to be captured in order to monitor structural health. The local phenomenon is captured by modes of higher frequency where as modes of lower frequency are employed for capturing global phenomenon material and geometry defects because of the reason that they are less sensitive to the local changes in the structure. Most researchers have presented ways and developed methods for low frequency devices where as the area of higher frequency devices for NDT is less explored which needs to be expedited for local phenomenon capturing occurring in the structures.

The objective of the thesis is to design and simulate a MEMS Energy Harvester which is helpful for Non-Destructive Structural Strength Monitoring of high frequency vibration structures having an additional capability of Temperature measurement. In this work a Cantilevered based Single layer Piezoelectric Energy Harvester along with Temperature Measuring Bimorph is proposed that is capable of producing up to 2 Volts of voltage at a frequency of 17761Hz when subjected to vibrations. The proposed energy harvester consists of a suspended piezoelectric mass with dimensions of $280\mu\text{m} \times 300\mu\text{m}$ and thickness of $4\mu\text{m}$ made up of PZT 5A (Lead Zirconate Titanate) material. Two bimorphs are attached on each side of the mass that bend due to the changes in the ambient temperature because of different coefficient of thermal expansion. The bimorphs show a displacement of $0\text{-}3\mu\text{m}$ for the temperature range of 295K to 337K .

It is shown through modeling and simulation (static and dynamic) that this device is viable option for use in structural health monitoring.

Key Words: *MEMS Energy Harvester, Non-Destructive Testing, High frequency structures, Piezoelectric Energy Harvester, Bimorph*

Table of Contents

Declaration.....	i
Language Correctness Certificate.....	ii
Copyright Statement.....	iii
Acknowledgements	iv
Abstract.....	vi
Table of Contents	vii
List of Figures.....	ixx
List of Tables	li

CHAPTER1: LITERATURE REVIEW

1.1	Motivation and Objective	1
1.2	Introduction	1
1.3	Non-Destructive Testing Methods/Techniques	2
	1.3.1 Visual Inspection	3
	1.3.2 Stress- wave methods for structures	3
	1.3.2.1 Ultrasonic Pulse Velocity Method	3
	1.3.2.2 Ultrasonic Echo Method	4
	1.3.2.3 Impact Echo Method	4
	1.3.2.4 Spectral Analysis of Surface Waves	4
	1.3.3 Stress-wave methods for deep foundations	5
	1.3.4 Nuclear Methods	5
	1.3.5 Electric and Magnetic methods	5
	1.3.6 Penetration method	5
	1.3.7 Infrared thermography	6
	1.3.8 Radar	6
1.4	Overview of Sensors Used in Structural Strength Monitoring	7
	1.4.1 Accelerometers	7
	1.4.1.1 Piezoelectric Accelerometers	7
	1.4.1.2 Piezoresistive Accelerometers	8
	1.4.1.3 Capacitive Accelerometers	8
	1.4.1.4 Servo Force Balance Accelerometers	8
	1.4.2 Strain Gages	9
	1.4.2.1 Electrical Resistance Strain Gages	9
	1.4.2.2 Vibrating Wire Strain Gages	9
	1.4.3 Displacement Sensors	10
	1.4.3.1 Linear Potentiometer	10
	1.4.3.2 Linear Variable Differential Transformers	10
	1.4.4 Tiltmeters and Inclometers	10

	1.4.4.1	Vibrating Wire Tiltmeter	10
	1.4.4.2	Electrolytic Tiltmeters	10
	1.4.4.3	Inertial Based Tiltmeters	11
	1.4.5	Acoustic Emission Sensor	11
	1.4.6	Fiber Optic Sensor	11
1.5		Significance of MEMS in Non-Destructive Strength Analysis	12
1.6		Significance of Energy Harvester in Non-Destructive Strength Analysis	13
	1.6.1	Piezoelectric Energy Harvesters	14
	1.6.2	Piezoelectric Energy Harvester Materials	16
1.7		Bimorph Temperature Sensors	16
1.8		Vibrational Frequency of Structures	17
CHAPTER2: DESIGN			
2.1		Piezoelectric Energy Harvester along with Temperature Sensor for High Frequency Applications	18
	2.2.1	Description of Design	18
		2.2.1.1 Anchor	19
		2.2.1.2 Energy Harvesting Part	19
		2.2.1.3 Bimorph Temperature Sensor	20
2.2		Mathematical Modeling	21
2.3		Properties of Materials Used in Design	23
CHAPTER3: SIMULATIONS			
3.1		Energy Harvester Design1 (Electrostatic)	25
	3.1.1	Simulation Results of Design1	25
3.2		Capacitive Energy Harvester Design (Design 2)	27
	3.2.1	Simulation Results of Capacitive Energy Harvester	28
3.3		Bimorph Piezoelectric Energy Harvester (Design 3)	31
	3.3.1	Simulation Results of Bimorph Piezoelectric Energy Harvester	31
3.4		Piezoelectric Energy Harvester with Temperature Sensor (Bimorph)	33
	3.4.1	Simulation Results, Static Analysis	34
	3.4.2	Frequency Analysis	36
	3.4.3	Harmonic Sweep Simulations	38
	3.4.4	Bimorph Portion Simulation Results	41
	3.4.5	Concrete Envelope Device Closure	44
CHAPTER4: RESULTS, DISCUSSION AND CONCLUSION			
4.1		Energy Harvester Design1 (Electrostatic)	46
4.2		Capacitive Energy Harvester Design (Design 2)	46
4.3		Bimorph Piezoelectric Energy Harvester (Design 3)	46
4.4		Piezoelectric Energy Harvester with Temperature Sensor (Bimorph)	47
4.5		Conclusion	50
CHAPTER5: FABRICATION TECHNIQUE AND FUTURE WORK			
5.1		Sputtering	51
5.2		Electron Beam Evaporation	52
5.3		Fabrication Steps	53
5.4		Future Work	55

List of Figures

Figure 2.1	Piezoelectric Energy Harvester along with Temperature Sensor for High Frequency Applications	18
Figure 2.2	Anchor	19
Figure 2.3	Piezoelectric Energy Harvester	19
Figure 2.4a	Bimorph Temperature Sensor	20
Figure 2.4b	Top View of Bimorph Temperature Sensor	20
Figure 2.5	Piezoelectric beam model	21
Figure3.1	Vibration based Energy Harvester	25
Figure3.1.1	Displacement results of the EH when subjected to small loads	26
Figure3.1.2	Stress values of the EH subjected to small mechanical loading	26
Figure3.1.3	Frequency Analysis of the energy harvester	27
Figure 3.2	Capacitive Energy Harvester Design	28
Figure3.2.1	Static analysis, Displacement of mass	28
Figure3.2.2	Static Analysis, Produced Voltage	29
Figure3.2.3	1 st Mode of Frequency	29
Figure3.2.4	2 nd Mode of Frequency	29
Figure3.2.5	3 rd Mode of Frequency	29
Figure3.2.6	4 th Mode of Frequency	29
Figure3.2.7	Temperature Effect on Device Especially on Springs	30
Figure3.2.8	Capacitance Results of Capacitive Energy Harvester	30
Figure3.3	Bimorph Piezoelectric Energy Harvester	31
Figure3.3.1	Static Analysis, Displacement of Piezoelectric Energy Harvester Cantilevers	31
Figure3.3.2	Frequency analysis of Piezoelectric Energy Harvester	32
Figure3.3.3	Voltage results of Piezoelectric Energy Harvester	32
Figure3.4	Cantilevered based Single layer Piezoelectric Energy Harvester along with Temperature Measuring Bimorph	33
Figure3.4.1	Static Analysis Displacement results for T=4um	34
Figure3.4.2	Static Analysis Voltage results for T=8um	34
Figure3.4.3	Graph showing displacement results of comparison for different thicknesses	35
Figure3.4.4	Graph showing voltage results of comparison for different thicknesses	35
Figure3.4.5	Frequency Analysis, Eigen Frequency results	36
Figure3.4.6	Frequency Analysis, Voltage Results at Frequency 17761Hz	37
Figure3.4.7	1 st Modal Frequency	37
Figure3.4.8	2 nd Modal Frequency	37
Figure3.4.9	3 rd Modal Frequency	38
Figure3.4.10	4 th Modal Frequency	38

Figure3.4.11	5 th Modal Frequency	38
Figure3.4.12	6 th Modal Frequency	38
Figure3.4.13	Applied Harmonic Pattern, 17500Hz	39
Figure3.4.14	Displacement Results	39
Figure3.4.15	Voltage at Harmonic Frequency 17500Hz	39
Figure3.4.16	Graph showing harmonic sweep results at different frequencies for displacement	40
Figure3.4.17	Graph showing harmonic sweep results at different frequencies for voltage	40
Figure3.4.18	Temperature Analysis, rise in temperature from 295K to 337K	41
Figure3.4.19	Temperature Analysis, Back view of the Device	41
Figure3.4.20	Deflection with rise of Temp	42
Figure3.4.21	Corresponding Displacement	42
Figure3.4.22	Back view of the Device	42
Figure3.4.23	Back view Displacement of Bimorph	42
Figure3.4.24	Voltage Vs Displacement Graph	43
Figure3.4.25	Corresponding Field Voltage	43
Figure3.4.26	Graph representing displacement of main mass with temperature rise	44
Figure3.4.27	Concrete Envelope around Device	44
Figure3.5.28	Effect of Increasing Temperature	45
Figure3.5.29	Effect on voltage due to rise in temperature corresponding to displacement	45
Figure4.1	Graph showing comparison of Theoretical calculations and simulation results for displacement of the device	48
Figure5.1	Silicon Deposition	53
Figure5.2	PZT Layer Deposition	53
Figure5.3a	Etching of PZT layer	53
Figure5.3b	A view from Anchor side	53
Figure5.4	Deposition of Ag layer	53
Figure5.5a	Patterning of Ag layer	53
Figure5.5b	View from anchor side	54
Figure5.6	Al layer deposition	54
Figure5.7a	Patterning of Al layer	54
Figure5.7b	View from anchor side	54
Figure5.8a	Back side Etching to free the device	54
Figure5.8b	View from Anchor side	54
Figure5.9	Anchor mask, Top view	55
Figure5.10	Bimorph mask, Top view	55
Figure5.11	PZT mask, Top view	55

List of Tables

Table 1.1	Comparison of Piezoelectric Energy Harvesters	15
Table 2.1	Poly Silicon material properties	23
Table 2.2	PZT 5A material properties	23
Table 4.1	Harmonic Sweep Results	49

CHAPTER 1: LITERATURE REVIEW

1.1 Motivation and Objective

Energy harvester is a device that can extract energy from the available ambient sources e.g. solar energy, mechanical vibrations, human body, thermal energy and electromagnetic energy etc. The feature of scavenging energy from such sources has become valuable and area of research with the development of micro-electro mechanical systems. MEMS devices are small in size, compact and can be embedded into the structures. Damage and Vibrations of a structure are a local phenomenon that appears in the structure (concrete/ mechanical) and this local phenomenon needs to be captured. The local phenomenon is captured by modes of higher frequency where as modes of lower frequency are employed for capturing of global phenomenon related to structures because of the reason that they are less sensitive to the local changes in the structure. Most researchers have presented ways and developed methods for low frequency devices where as the area of higher frequency devices for NDT is less explored which needs to be expedited for local phenomenon capturing occurring in the structures. The objective of the thesis is to design and simulate a MEMS Energy Harvester which is helpful for Non-Destructive Structural Strength Monitoring of high frequency vibration structures having an additional capability of Temperature measurement.

1.2 INTRODUCTION

Structures, whether concrete or mechanical are combinations of elements and parts build together to withstand loads they are designed for which further transfer the load to the foundations. Quality and strength of material used to construct such structures is considered the basis of effectiveness and durability for the structure. Hence the standard and most taken care of property is the quality of the material being used for the purpose of construction. With the passage of time these structures start to deteriorate and the useful life begins to diminish rapidly. The strength monitoring of old along with that of new structures is imperative with characterization of material properties and natural impacts that are turning in to a genuine concern. Hence methods are devised for the analysis of structure to estimate their useful life span and continuously monitor their condition using the established methods.

Non-Destructive strength analysis is one of the established methods that are most widely used for analyzing the behavior of the structure. By Non-destructive methods it is meant that the structure

would be subjected to such testing procedures which leave the structure unharmed and un-deteriorated i.e. no effect on the health of structure. Nondestructive Testing (NDT) assumes a vital part in guaranteeing that concrete and mechanical parts perform to their capacity in a sheltered, solid, and savvy way. NDT professionals perform the important tests to find the defects and discontinuities that may bring about deterioration or collapse in such frameworks. These tests are performed in a way that does not influence the future effectiveness of the subject under test thus, the name "nondestructive." NDT takes into account watchful and careful materials assessment without the requirement for deconstruction or harm. NDT has become part of section's life cycle as it is regularly employed to recognize deterioration of structures caused due to the maintenance related conditions of the structure wear, fatigue, attrition, agitation or different components which persistently influence quality [1].

The nature of new concrete solid structures is subject to numerous variables, for example, sort of concrete, kind of cumulative material, water bond proportion, curing, ecological conditions and so forth. Other than this, the control practiced amid development additionally contributes a considerable measure to accomplish the sought quality. The present arrangement of checking slump and testing solid shapes, to evaluate the quality of solid, in structure under development, are not adequate as the genuine quality of the structure rely on numerous different elements, for example, fitting compaction, viable curing moreover. Considering the above necessities, need of testing of solidified solid in new structures as well as old structures, is there to assess the genuine state of structures. Non-Destructive Testing (NDT) systems can be utilized successfully for examination and assessing the genuine state of the structures. These systems are generally brisk, simple to utilize, and shabby and give a general evidence of the obliged property of the cement.

1.3 Non-Destructive Testing Methods/ Techniques

Many non- destructive testing methods/ techniques have been developed to analyze structures including wired along with wireless techniques. Some of the methods are summarized in the following paragraphs along with a brief description of the principle used

1.3.1 Visual Inspection

1.3.2 Stress- wave methods for structures

1.3.3 Stress-wave methods for deep foundations

1.3.4 Nuclear Methods

1.3.5 Electric and Magnetic methods

- 1.3.6 Penetration method
- 1.3.7 Infrared thermography
- 1.3.8 Radar

1.3.1 Visual Inspection

Visual inspection being the first most and primary method of the inspection of structures involves inspecting the structures visually using all the related experience gained throughout the years. It involves observing the structure, documenting and classifying the appearance of the structure involving distresses on the surfaces that are exposed and damage inferred to the structure etc. Visual review can give a qualified specialist with an abundance of data that may prompt positive recognizable proof of the reason for the observed trouble. Expansive information in auxiliary designing, solid materials, and development systems is expected to concentrate the most data from the visual investigation. These reports give data for perceiving and characterizing diverse sorts of harm, furthermore can help to distinguish the reasonable justification of the damage.

Visual assessment is one of the most flexible and capable NDT routines. On the other hand, as said over, its viability relies on upon the information also, experience of the agent. Visual examination has the undeniable confinement that just unmistakable surfaces can be assessed. Inward abandons go unnoticed and no quantitative data is acquired about the properties of the cement. Therefore, a visual review is generally supplemented by one or a greater amount of the other NDT routines involving optical magnification, stereo microscope, fiberscopes, borescopes and digital video camera [2].

1.3.2 Stress Wave Method

The method originally takes advantage of ultrasonic and impact waves and the corresponding measurement of these waves to inspect the structure. Ultrasonic pulse velocity, Ultrasonic echo, Impact echo and spectral analysis of surface waves make up the stress wave method [3]. A brief description is as under

1.3.2.1 Ultrasonic Pulse Velocity Method

It is one of the oldest NDT method in which the velocity or travel time of the wave is calculated by sending a pulse of compressed ultrasonic waves over a known length of path i.e. through the structure and verily also known as ultrasonic through transmission and ultrasonic pulse velocity method. The speed of proliferation of these waves relies on upon the thickness and the elastic constants of the solid. In a solid part, varieties in thickness can emerge from non-uniform combination, and varieties in elastic properties can happen because of varieties in materials, blend

extents, or curing. Accordingly, by deciding the wave speed at diverse areas in a structure, it is conceivable to make derivations about the consistency of the cement. The compressional wave rate is dictated by measuring the travel time of the wave over the known length of the path or known distance [3] [4].

1.3.2.2 Ultrasonic Echo Method

In this method ultrasonic echo is monitored once the transmitted ultrasonic wave gets reflected from a defect or unsmooth surface. The waves are injected into the structure using a transmitter and reflected waves are received by the receiver. The key segments of an ultrasonic echo test framework are the transmitting and receiving transducer(s), a pulser, and an oscilloscope. An ultrasonic wave is presented into the subject structure at an open surface by a transmitter.

The stress wave spreads into the structure and is reflected by defects or interfaces. The surface reaction brought about by the landing of reflected waves, or echoes, is checked by the same transducer going about as a receiver. The recipient yield wave is shown on an oscilloscope as a period space waveform. The round-excursion travel time of the stress wave can be calculated from the waveform by deciding the time from the begin of the transmitted wave to the gathering of the echo. In the event that the wave speed in the material is known, this travel time can be utilized to focus the depth of the reflecting interface [3] [5].

1.3.2.3 Impact Echo Method

In this method the echo is monitored when the reflected impact wave is received at the receiving end. The impact is generated by the mechanical means which travels all along the structure and the reflected waves received may be in numbers depending upon the defects inside the structure. A transient stress wave is presented into a structure by mechanical means/ impact. The P- and S-waves delivered by the stress waves spread into the subject structure along hemispherical wavefronts. Moreover, a surface wave goes along the surface far from the effect point. The waves are reflected by inner interfaces or outer limits. The entry of these reflected waves, or echoes, at the surface where the effect was produced produces echo that are measured by an accepting transducer and recorded utilizing an information securing framework. Understanding of waveforms in the time space has been fruitful in seismic-echo applications including long slim structural members such as bored shafts and piles [5].

1.3.2.4 Spectral Analysis of Surface Waves

Stress waves are generated in the structure by impact and two receivers are used to monitor the reflected wave along the surface. The received signals are developed and an ensuing computation

plan is utilized to deduce the stiffnesses of the hidden layers. Usually this technique is feasible for detection of depth damage [6].

1.3.3 Stress Wave Method for deep foundations

The principle of operation depends upon the propagation of stress wave and suitable for strength analysis of deep foundations as it utilizes Sonic echo, Impulse response, Impedance logging, Cross hole sonic logging and Parallel seismic techniques for the detection of defects in the structures and drilled shafts, hence basically depending on reflection techniques and direct transmission techniques. The working principle is quite obvious that the stress wave is propagated into the structure and using the travel time of the reflected wave through the deep foundations defects are detected. In some methods various parallel metal plastic tubes are placed in the structure before cement settles down, or center gaps to be bored after the cement has set. A transmitter test put at the base of one tube discharges a ultrasonic stress wave that is recognized by a collector test at the base of a second tube. A recording unit measures the time taken for the ultrasonic stress wave to go through the cement between the tubes [7].

1.3.4 Nuclear Methods

Nuclear method comprises of Direct transmission radiometry, Back scatter radiometry, Radiography and Gamma gamma logging. The working principle of nuclear methods depends upon the interaction between high energy electromagnetic radiations and the subject structure. The interaction between these two reveals the state of the structure during early period when concrete is hardening to the period the structure is near the completion of its life span. Wide range of information is made available using the technique [8].

1.3.5 Electric and Magnetic Methods

Learning about the amount and area of support is expected to assess the quality of fortified cement structures. Knowing whether there is dynamic erosion of fortification is important to evaluate the requirement for activities before basic security or serviceability is endangered. Comprising of Covermeter, Half cell potential and Polarization methods electric and magnetic methods provide with necessary information required for analyzing the structure in detail [9].

1.3.6 Penetration Method

Penetrations method is based on water absorption, water permeability and air permeability tests to render the required information from the structure under observation. Huge numbers of the corrosion mechanism in concrete include the entrance of forceful materials for example, sulfates, carbon dioxide, and chloride particles. In most cases, water is likewise needed to support the

debasement instruments. Thus, solid that has a surface zone that is exceedingly impervious to the entrance of water will by and large be strong. The capacity of cement to withstand ecological weakening relies on the materials that were utilized to make the concrete, the blend extents, the level of union, furthermore, the curing conditions. The nature of the surface zone has been progressively recognized as the central point influencing the rate of corruption of a solid structure. To survey the potential toughness of set up solid, it is important to concentrate on techniques that evaluate the capacity of the surface zone to limit the entry of outside operators that may prompt direct decay of the cement or to depassivation and erosion of implanted support [10].

1.3.7 Infrared thermography

Infrared thermography may be thought of as thermal imaging. The thermal radiations coming out of the structure are taken care of or heat flow disturbance on the surface of the structure reveals the condition of the subject under observation. Obviously these are temperature dependent and the basic requirement is temperature change measurement. Infrared thermography detects the discharge of thermal radiations and produces a visual picture from this radiation as the surface emits electromagnetic radiation energy [11]. Thermography, similar to any framework utilizing infrared radiation, measures variety in surface warmth and does not specifically measure surface temperature. So it can be utilized to recognize abnormalities in surface temperature that may be used to identify the subsurface defects (due to the difference of the temperature in the surfaces) and the state of the solid material.

1.3.8 Radar

Electromagnetic radiations are used instead of stress waves as done in pulse echo technique. The technique is useful in locating voids, thickness, identifying deterioration and reinforced bars. A radio wire (antenna), which is either dragged over the surface or appended to a review vehicle, transmits short beats of electromagnetic energy (inside of a particular expansive recurrence band) that enter into the reviewed material. The most generally utilized waves for solid assessment range from 1 to 3 nanoseconds (n sec) in span and frequently contain three or four crests. Investigation and elucidation of the sign is in light of all around characterized ostensible focus recurrence values, most normally between 500 MHz and 1 GHz for basic reviews. Every wave goes through the material; a part of the wave energy is reflected back to the reception apparatus at the point when an interface between materials of different dielectric properties is experienced. The antenna gets the reflected energy and creates a yield signal corresponding to the amplitude of the reflected

electromagnetic field. The received signal therefore contains data on what was reflected, how rapidly the signal jaunted back, and how a significant part of the signal was weakened [12].

1.4 Overview of Sensors used in Structural Strength Monitoring

All the methods that have been discussed earlier require some values or data from the structure in order to approximation the damage incurred to the structure by observing the information values gathered from the structure. Despite the fact that a some of the strategies discussed just oblige information from visual or manual investigation, this kind of information is tiresome and expensive to acquire. As a result of this issue, most research in the area of structural strength analysis has been concentrated on the utilization of sensor frameworks to gather the vital data for examination. Mainly environmental and kinematic quantities are of much concern during the analysis of the structure e.g temperature, humidity, Ph, force, stress, strain, displacement, vibrations, moisture content etc are the quantities that are required for the proper analysis of the health and state of the structure [13] [14].

The following section introduces the most usually utilized sensors which have been developed, checked and tested vigorously along with some advanced sensor technologies being recently developed and in use, yet this list is by no means a complete presentation of the sensors developed for the cause.

1.4.1 Accelerometers

Accelerometers are devices (sensors) that are employed to measure the acceleration of a structure at some specific area which are created due to some mechanical force, load or gravity. These accelerations may appear as vibrational measurements. Frequency, damping and mode shapes are such attributes of the structure that can be calculated through post measurement using accelerometers and are helpful in depicting the state. Most commonly used accelerometers are briefly discussed as under.

1.4.1.1 Piezoelectric Accelerometers

These sensors work on the principle of piezoelectricity i.e. generation of voltage due to some mechanical force being experienced. Piezoelectric element and seismic mass are the most important components in the said accelerometers. These sensors are attributed with wide frequency range operation, high output, durability and optimum size. Acceleration is applied to the base of the sensor; the piezoelectric components encounter a force parallel to the mass they are joined with

and subsequently to the vibrations being experienced. This power makes an electrical yield that can be sent through a link to a information obtaining framework where it can be prepared further. A critical favorable position to these sorts of sensors is that they are self-creating. The piezoelectric material yields an electrical output without the need of a consistent electrical or force source. At the point when this sort of accelerometer was initially imagined, it obliged extraordinary low noise cabling to counter the fact of noise and environmental interruption effects that were susceptible to add up in the original signal being transmitted. Piezoelectric accelerometers are mainly operated in three modes namely shear mode, flexural mode and compression mode [13].

1.4.1.2 Piezoresistive Accelerometers

The accelerometers that operate on the principle of piezoresistivity fall under this category. Piezoresistive effect only changes the conductor or semiconductor's electrical resistivity and not having any effect on electrical potential. When a mechanical force or load is applied the resistivity of the conductor/semiconductor is changed due to the piezoresistivity effect. The strain gages use resistors made of single-gem silicon. The electrical resistance of this material changes in extent to the excitation signal or power connected to it. The normal structure of piezoresistive accelerometers includes these strain gages appended to a cantilever beam with a seismic mass connected. As the sensor encounters vibrations or acceleration, stress in strain gages change which modifies the electrical signal yielded by a Wheatstone extension circuit [13].

1.4.1.3 Capacitance Accelerometers

The mode of operation is similar to that of piezoresistive accelerometers as capacitance accelerometers measure a change in capacitance rather than the change in resistance. A capacitive accelerometer is a kind of accelerometer device that measures the vibrations/ acceleration on a surface utilizing capacitive detecting methods [13]. It can sense dynamic and static stepping on hardware or gadgets produced due to mechanical means and consequently changes over this acceleration up into electrical streams or voltage.

1.4.1.4 Servo Force Balance Accelerometers

Servo force balance accelerometer makes use of electromagnetic forces to move an internal capacitor plate in such a way that the seismic mass keeps its neutral position sustained. This electromagnetic force is proportional to the acceleration that is experienced by the sensor [13]. The operation of this sensor happens quickly enough that there is for all intents and purposes no

relative displacement between the plate and the backings which lessens the impacts of nonlinearities that can happen with the other three sensors.

1.4.2 Strain Gages

The working principle of strain gages is quite simple and easy. They measure the strain at a location inside the structure where these are installed by changing the load path making a detectable difference in the distribution of strain. The best point of interest of these sensors is that they are economical and simple to install. Although strain gages can just gauge the strain of a structure at one area, the data picked up from these sensors can be utilized with a limited component model of the structure to help distinguish when harm may have happened [13]. The utilization of strain gages in this sort of strategy is based upon the rule that damage to basic area will prompt an adjustment to the load and hence a noticeable contrast in strain dissemination.

The most commonly used strain gages are briefly discussed below:-

1.4.2.1 Electrical Resistance Strain Gages

The principle working behind this type of strain gage is the change in resistance of the conductor due to the stress experienced by the sensor. Conducting material's resistance (electrical resistance) is inversely proportional to the area and proportional to the length and amount of stress may be inferred by measuring the electrical resistance of the gage which increases as the strain is increased and vice versa. A strain gage exploits the physical property of electrical conductance and its reliance on the conduit's geometry. At the point when an electrical conductor is extended inside of the points of confinement such that it doesn't break or fall twist, it will get to be smaller and more, changes that build its electrical resistance end-to-end. At the point when the strain gage is joined and reinforced well to the surface of structure, the two are considered to deface together. The strain of the strain gage wire along the longitudinal heading is the same as the strain on the surface in the same direction.

1.4.2.2 Vibrating Wire Strain Gages

An electromagnetic coil excites the wire as a pre-tensioned steel wire is fixed at the supports encased within a steel tube to read its natural frequency. It is another popular method that is used for measuring strain. A steel wire being tensioned between two end blocks that are embedded directly in the structure causes the end supports to move relative to each other due to the excitation of electromagnetic coil which alters the tension in the steel wire and can be calculated by measuring the resonant frequency.

1.4.3 Displacement Sensors

The working principle of these sensors is quite clear from the name of the sensors as one of the parameters namely displacement is monitored. The most commonly used two displacement sensors are linear potentiometers and linear variable differential transformers.

1.4.3.1 Linear Potentiometers

Linear potentiometers also called cable extension transducers, are included a spool with a length of stainless steel link twisted on it, a strain spring that keeps the spool stacked so that either heading of displacement can be measured, and an accuracy potentiometer. Moreover, the primary lodging of the sensor is appended to a fixed place, with the end of the link associated with the part or segment whose displacement is being checked. As the area of interest uproots, the link reaches out from or withdraws onto the spool which pivots. The pivot of the spool moves the potentiometer. A potentiometer comprises of a slight film resonator with a mobile wiper which is in contact with the electrical resistor. As the wiper moves over the resonator because of the revolution of the link spool, a change in electrical resistance happens which is relative to the removal of the link.

1.4.3.2 Linear Variable Differential Transformers

The working principle is based on the principle of mutual induction. A moveable magnetic core with two hollow metallic cylinders which comprise of the primary and the secondary coil as voltage is applied to the primary coil consequently same is induced in the secondary coil due to mutual induction, the magnetic core displaces and this displacement is being monitored.

1.4.4 Tiltmeters and Inclinometers

These sensors are of interest as tilt or slope of a particular location is monitored utilizing this sensor. The three types of tiltmeters used are briefly discussed as under [14]

1.4.4.1 Vibrating Wire Tiltmeter

It comprises of a supported vibrating wire strain gage along with a pendulous mass. Due to the rotation because of the tilting of the sensor, the mass upon the strain gage changes due to the gravitational force. The frequency gets changed due to the change in position of vibrating strain gage and hence the relationship between the angle of rotation and frequency can be determined.

1.4.4.2 Electrolytic Tiltmeters

Electrolytic tiltmeters use a high-accuracy electrolytic tilt transducer and the essential detecting component. These gadgets are energized by an AC motion through the tilt transducer, and as the transducer tilts, inside cathodes are secured or revealed by a conductive liquid inside of the gadget. As these terminals are uncovered or expelled from the conductive liquid, the electrical

imperviousness to the excitation sign is modified which can be changed over to an adjustment in edge through a scaling element.

1.4.4.3 Inertial Based Inclinometers

Inertial based inclinometers are the primary choice for measuring element tilt changes. The innovation in these gadgets is like that of a servo force balanced accelerometer. These inclinometers additionally contain a pendulous mass, and the movement of this mass is distinguished by an optical position sensor. The perusing from this position sensor is contrasted with the first state and an adjusting current is delivered and connected to a torque engine to give back the mass to the first state.

1.4.5 Acoustic Emission Sensor

The most widely recognized kind of acoustic emission sensor utilizes piezoelectric materials like the operation of a piezoelectric accelerometer. This kind of sensor has been ended up being more tough and delicate than different strategies based upon capacitance or laser-optics. The piezoelectric material inside the sensor encounters the power from the stress waves proliferating from a break and yields a relative electrical signal or voltage [14]. A fundamental outline of an acoustic emission sensor. All together for these sensors to be appropriate, they are ordinarily utilized inside of a system of different sensors so triangulation can be performed to focus the area of a stress wave source. The best points of interest of acoustic emission sensors is the capacity to distinguish damage as it happens and the way that the damage does not have to happen at the site of the sensor for it to be recognized. Steel is the best material for the utilization of acoustic emission sensors in light of the fact that the stress waves don't ease as severely and can be identified at long distances.

1.4.6 Fiber Optic Sensors

Fiber optic sensors are generally new innovations that have a lot of promising applications. The fundamental operation of these sensors includes sending light beams down a fiber optic link at consistent interims and measuring the progressions/reflections that happen as this light is reflected. Four types of standards sensors are usually used to decode these light signal i.e. interferometry, polarization, spectroscopy, and light power. Interferometry based fiber optic sensors measure environmental changes by monitoring the change in the shape of the light waves [14]. At the point when the standard of polarization is utilized, the progressions in optical polarization of a light signal are the measure of interest . A standout amongst the most widely recognized sorts of fiber optic sensor sorts is a fiber Bragg grating sensor which is taking into account the standard of

spectroscopy. They monitor the change in reflected light source wavelength. Sensors utilizing the standard of light energy measure how light intensity changes over the length of a fiber.

1.5 Significance of Micro Electro Mechanical System (MEMS) in Non-Destructive Strength Analysis

Micro Electro Mechanical Systems (MEMS) is a blend of mechanical engineering and semiconductor processing at very small level producing electro mechanical systems capable of sensing and actuating systems depending upon the application being utilized in. MEMS are the coordination of mechanical components, for example, sensors and actuators with gadgets on a typical silicon substrate through usage of microfabrication technology. In the most fundamental framework, the sensors accumulate data from environment through measuring mechanical, synthetic, organic, chemical, biological, optical and magnetized phenomena, the hardware then prepare the data got from the sensors and henceforth guide the actuators to react by moving, situating, directing, pumping and separating, keeping in mind the end goal to control the phenomenon being monitored [15].

The past couple of years have seen remarkable progress in micro-electro-mechanical systems frameworks (MEMS) and microsensors. Advancements in designing and fabrication of embedded microdevices has set MEMS to enter into civil infrastructure monitoring with sustainability and availability of wireless data communication networks. MEMS innovation allows the formation of micromechanical transducers to transform chemical and physical stimulus into electrical signals i.e. voltage. Advances in MEMS additionally permit these devices to be small in size and sufficiently rugged to be distributed all through a structure in numbers from hundreds to millions.

The issues in non-destructive testing of structures can be directly solved by observing vibrations, temperature, dampness, pH and chloride fixation in the structure utilizing relating MEMS sensors and devices. A few components dominate others in effect of deterioration of health and subsequently more critical to screen than the rest. MEMS is becoming pretty much popular in the area of non-destructive testing of structures because of the amazing features, small size, robust and high outputs and at times using the environmental energy to power the micro devices. Acoustic emission (AE) checking of structures includes instrumenting the picked structure furthermore, "listening" for trademark signals. AE are the versatile strain waves created by quick discharge of energy among split stimulating and inner distortions in materials. This arrival of energy is showed as transient stress waves which spread outwards from the locus of an auxiliary change got on by changes the neighborhood anxiety field. These separations are basically prompt and can be

delivered by such fluctuated causes as split nucleation and development, influencing inter surface slippage, twinning, stage changes, plastic distortions, and microseismic movement. High-fidelity MEMS-AE are required so recorded signals can be contrasted with the hypothetical waveforms expected for different sorts of defects, permitting the sensor to choose whether the occasion is from important material or natural commotion. This significantly diminishes the need of information to be exchanged over the array network, permitting unambiguous real time detection of damaged areas.

Accelerometers are utilized to detect acceleration. These gadgets regularly monitor the proof mass displacement due to the vibrations /accelerations. MEMS accelerometers are currently accessible with differing accuracy from 2 G to 50 G and in one, two, or three axis models.

There are three fundamental sorts of electrical temperature sensors: thermocouples, resistive temperature devices (RTD), and thermistors. Thermocouples determine temperature because of voltage produced at a contact pad between two distinctive metals. RTDs and thermistors both depend on electrical resistance in the materials due to the temperature dependency. RTDs and thermistors are commercially available in integrated circuits (IC) structure with on-chip compensation, buffering, and linearization hardware [15] [16].

Stickiness and dampness (Moisture and Humidity) detecting are commonly done utilizing a capacitive arrangement of metal anodes sandwiching a polymer. The dielectric properties of the polymer differ discernibly with changes in dampness. Sensors for distinguishing pH have been created utilizing thick film technology to build multi-layer structures comprising of a conductor and interfacial layers on an alumina ceramic substrate. This sort of microsensor is not yet industrially accessible.

1.6 Significance of Energy Harvesters in Non-Destructive Strength Analysis

The utilization of remote sensors and embedded medicinal electronic frameworks have rapidly grown to high extent in few past years. They are normally controlled by standard batteries which get to be exhausted inside in a moderately short time, yet the substitution or replacing of batteries is a significant bottleneck for wide consumption of remote sensor hubs (WSN). Additionally, while the span of electronic hardware has contracted on account of the appearance of incorporated circuit innovation, batteries are these days regularly the most cumbersome gadgets in remote sensor hubs. With the latest advances in remote and micro electromechanical systems (MEMS) innovation, the interest for convenient hardware and remote sensors is rapidly increasing [17]. Since these gadgets are compact, it gets to be essential that they convey their own particular power supply. As a rule

this force supply is the regular battery; in any case, issues can happen when utilizing batteries due to their limited lifespan. For convenient gadgets, replacing the battery is tricky in light of the fact that the hardware could pass on whenever and substitution of the battery can turn into a monotonous assignment. On account of remote sensors, these gadgets can be set in exceptionally remote areas, for example, basic sensors on an extension or worldwide situating framework (GPS), GPS beacons on bridges [16] [18]. At the point when the battery is overpowered of all its power, the sensor must be recovered and the battery replaced. Due to the remote situation of these gadgets, getting the sensor out to replace the battery can turn into an extremely costly assignment or even incomprehensible [19] [20]. For example, in common framework applications it is frequently appealing to implant the sensor, making battery substitution unfeasible. In the course of time scavenging energy in the encompassing medium could be acquired, then it could be utilized to change or charge the battery [21].

1.6.1 Piezoelectric Energy Harvesters

One system is to utilize piezoelectric materials to acquire energy lost because of vibrations of the structure. This caught energy could then be utilized to increase the lifespan of the device/power supply or either be utilized to deliver constant energy to the electronic device. Consequently, the measure of exploration dedicated to power harvesting has been rapidly expanding. Vibration-based MEMS power generators display an astonishing answer for supply control for remote sensor hubs, which can create mW or μ W level power. Vibration energy scavenging has been exploited for transducing ambient energy into electric energy by a few distinctive transduction systems, including piezoelectric, electromagnetic and electrostatic strategies. Among these three energy scavenging techniques, the piezoelectric energy harvesting (PEH) has a high electromechanical coupling impact, and obliges no outer voltage sources. MEMS technology has been widely employed for the fabrication of energy harvesters to power up micro devices or useful battery options.

The examination of energy transformation procedures using surrounding vibrations has been of remarkable interest for some researchers for over a decade or two, although most advancements of installed piezoelectric structures have concentrated on applications of crack discovery utilizing screw disengagement and incorporation systems and health monitoring, furthermore, control frameworks, the latest utilizations of piezoelectric gadgets have likewise included the transformation of ambient vibration into low electrical power. The energy separated from vibrating

gadgets and structures can be used for driving electronic gadgets, supplying direct present into rechargeable batteries or electrical power supply gadgets. One of numerous applications being considered is for driving intense remote sensor gadgets. The utilization of piezoelectric material in the utilization of energy transformation obliges learning of scientific techniques, circuit segments, material properties and geometrical structure. The real advantages of piezoelectric transduction have demonstrated sensible prospect for self-symptomatic discovery of air ship sensor systems, microelectromechanical framework routine, conservative design, high affectability as for low info mechanical vibration and is suitable to be utilized right now or installed with different substructures presently other transduction methods. The piezoelectric vibration based energy harvesters can be incited as an outcome of the information vibration creating the subsequent electrical field. The resultant removed electrical energy can be advanced by using an electronic circuit equipped for supplying the immediate current into a rechargeable battery for the use of remote sensor correspondence. MEMS energy collector is a promising substitute for battery, particularly in low power utilization applications, for example, remote sensor systems and biomedical implantable gadgets. There are numerous energy sources in the environment, for example, low recurrence vibration, sunlight based energy and wind energy. Contrasted with different sorts of energy, vibration is practically accessible all over and can be effortlessly changed over to electrical power by electromagnetic.

The MEMS piezoelectric energy harvesters which appear in the literature have an output ranging from $0.85\mu\text{W}$ to $70\mu\text{W}$ and voltage outputs ranging up to 3Volts. A comparison is tabulated below in table 1.1.

S. No.	Author	Size	Frequency	Voltage Output	Power
1.	Renaud et al. [22]	1.5mm x 5mm	1.8KHz	-----	$40\mu\text{W}$
2.	Jeon et al. [25]	$170\mu\text{m} \times 260\mu\text{m}$	13.9KHz	2.4V	$1\mu\text{W}$
3.	Fang et al. [23]	$2000\mu\text{m} \times 500\mu\text{m}$	609Hz	-----	$2.16\mu\text{W}$
4.	Muralt et al. [24]	$800\mu\text{m} \times 400\mu\text{m}$	870Hz	1.6V	$1.4\mu\text{W}$
5.	Hua Yu et al. [23]	0.8mm x 1.24mm	235Hz	-----	$66.75\mu\text{W}$

Table 1.1: Comparison of Piezoelectric Energy Harvesters

1.6.2 Piezoelectric Energy Harvester Materials

Piezoelectric transducers make utilization of electrically captivated materials, for example, Barium Titanate (BaTiO_3), Zinc Oxide (ZnO) and Lead Zirconate Titanate ($\text{Pb}[\text{Zr}_x\text{Ti}_{1-x}]\text{O}_3$), generally known as PZT and suitable for high electromechanical pairing. Lead Zirconate Titanate PZT-5A has higher output compared to other materials and material properties are well suited for energy harvesting that is why it is preferred for energy scavenging. Piezoelectric transducers are equipped for high voltage level (from 2 to a few volts), all around adjusted for reduced size and great in delivering force thickness per unit volume [26] [27]. The real advantages of piezoelectric transduction have demonstrated tremendous prospect for self-symptomatic discovery of airplane sensor systems, micro-electromechanical framework configuration, dense arrangement, high affectability concerning low mechanical input vibrations and is suitable to be utilized or installed with different substructures compared to other transduction techniques. However, piezoelectric coupling drops off quickly at micrometric scale and moderately huge impedances are needed to achieve the most favorable working position. Furthermore, different issues must be viewed as, for example, time, depolarization and fragility. For low recurrence applications, like those identified with wearable sensors, polymer-based materials (e.g. dielectric elastomers) constitute a substantial distinct option for ceramics in light of their adaptability, reasonability and solidness [28] [29] [30].

1.7 Bimorph Temperature Sensors

Bimorphs are two metallic surfaces connected together which move upwards or downwards depending upon coefficient of thermal expansions of the metals joined together. As the temperature changes (increase or decrease) from the relative temperature i.e. the temperature at which the two metals were bonded together to make a bimetallic strip, a shearing force is experienced by the strip and hence it moves according to the coefficient of thermal expansion of the bonded metals. A micro cantilever based sensor can identify exceptionally small changes in temperature and surface stress changes. It has discovered a few applications in thermal, infrared biological, chemical and organic detecting. The resonance frequency change or static deflection of the sensor indicates the changes in the temperature. Diversion detecting routines can be partitioned into two classes: electrical and optical. Despite the fact that the electrical technique, including capacitance and piezo-resistive detecting, is promising because of its similarity with electric signal preparing, it is restricted because of absence of thermal detachment and Johnson clamor. Moreover, for piezo-resistive detecting, there are mechanical cutoff points in creating a flimsy, extremely sensitive cantilever.

The bimetallic effect is presently utilized as a part of various applications going from residential apparatuses to compensation in satellites. The said effect can be utilized as a part of two courses: either at this very moment actuator or as a temperature sensor. A bimetallic actuator comprises of two metal strips settled together. In the event that the two metals have distinctive CTE's then at this very moment the temperature of the actuator changes, one component will grow more than the other, creating the gadget to curve out of plane. The most widely recognized readout strategies for cantilever movement are optical including optical lever and interferometric routines. These optical techniques can recognize cantilever movement with sub-Angstrom determination constrained just by observing thermal vibrational characteristics.

1.8 Vibrational Frequency of Structures

Vibration can be characterized in respect of the quantities like acceleration, velocity and displacement. It is basically an oscillatory movement due to the different forces i.e. varying forces acting on a structure. Vibrations can be occasional, stationary irregular, non-stationary arbitrary and transient. Conventional mechanical tripout gadgets, for example, the spring based magnetic holding types, are acceleration sensors. These are activated by changes in the vibration power at the extent. At low frequencies these gadgets are seriously constrained on the grounds that due to frequency based acceleration decrement and to trip the sensor large displacements are needed in order to generate adequate accelerations.

The examination of particular frequencies of the most critical amplitudes makes it conceivable to figure the dynamic versatile module E_{dyn} and the Poisson proportion ν , by utilizing the densities measured on the section. For example, the recorded frequencies for the cement G8 in soaked conditions are 6357, 9663, 14934 and 19800. In rotary machines, the vibrations are caused due to the very reason of mechanical deprivation the mechanical strength of the gadgetry is observed by measuring these vibrations. Frequency and amplitude are the attributes for measuring vibration. The range of the vibrations that arise in compressors, turbines, and other rotational equipment is by and large somewhere around 10 and with extreme values falling somewhere around 20,000 Hz [31] [32].

CHAPTER 2: DESIGN

Piezoelectric Energy Harvester along with Temperature Sensor for High Frequency Applications is presented in Figure 2.1 that shows pictorial view of the piezoelectric energy harvester along with temperature sensor for high frequency applications. The central mass consists of lead zirconate titanate (PZT 5A) the piezoelectric material, anchor is made up of Silicon where as the side arms in the figure represent bimetallic strip i.e. bimorph which is designed for temperature measurement due to bending or deflection as the temperature is increased.

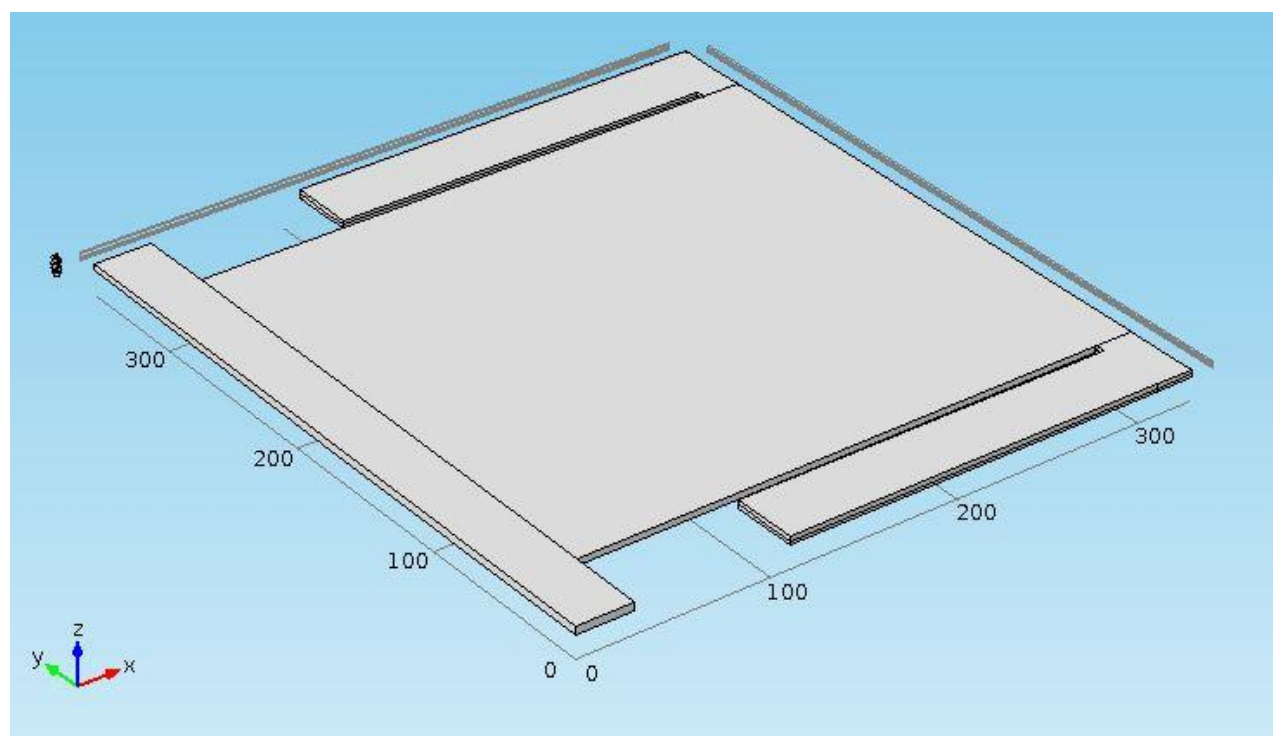


Figure 2.1: Piezoelectric Energy Harvester along with Temperature Sensor for High Frequency Applications

2.1 Description of Design

The designed piezoelectric energy harvester with bimorph temperature sensor for high frequency structures (concrete plus mechanical) is presented in figure 2.1 which is having a length of 330 μm , width 360 μm and thickness of 4 μm . The designed energy harvester consists of mainly three parts

1. Anchor
2. Piezoelectric Energy Harvester
3. Bimorph Temperature Sensor

Detail of each is as under

2.1.1 Anchor

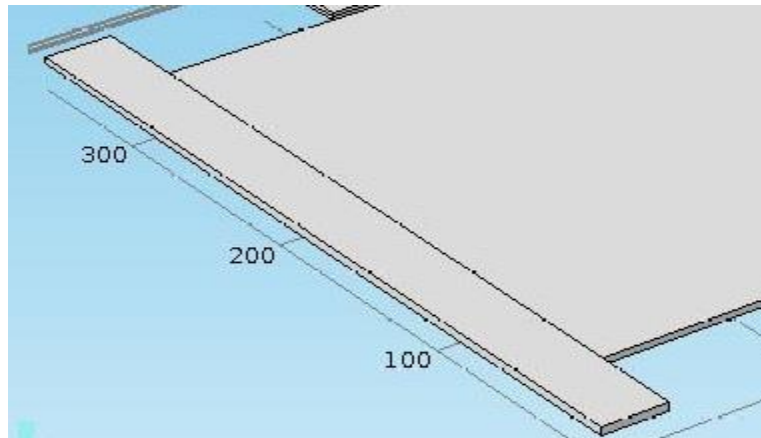


Figure 2.2: Anchor

Anchor is a firm support that is designed to hold the rest of the structure of the device in order to provide stability and firmness. Anchor remains fixed in its place and carry the whole device especially in a cantilevered structure as also depicted in this design also. Device performance is also based on the anchor rigidity or flexibility especially resonant frequency, displacement and stiffness are most affected entities. In the above design (figure 1) anchor is used as a support for the energy harvester. Another view is shown in figure 2.2 depicting anchor as a support to the main mass of the device. Anchor is 360 μm long, 30 μm wide and 4 μm thick made up of Silicon.

2.1.2 Energy Harvesting Part

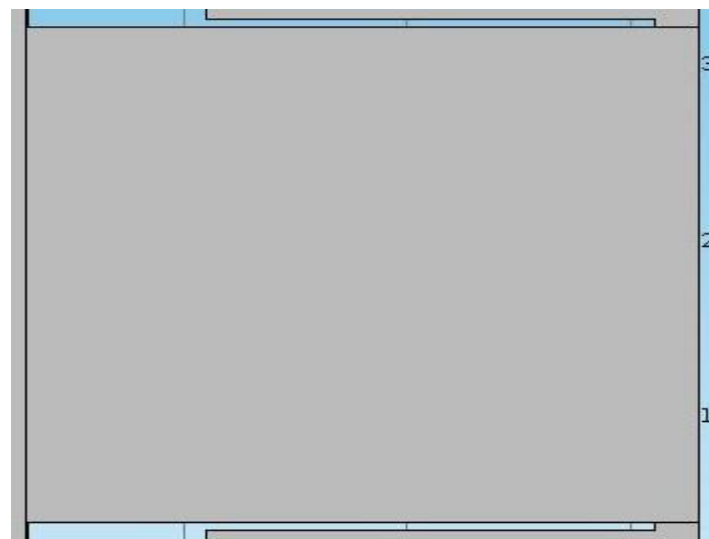


Figure 2.3: Piezoelectric Energy Harvester

Energy harvesting part is shown in figure 2.3. It consists of a piezoelectric material PZT-5A known as Lead Zirconate Titanate. The basic idea is utilizing the piezoelectric effect for the production of

electrical quantities i.e. voltage in specific. A mechanical force or pressure is applied on the piezoelectric material i.e. the material is squeezed mechanically and in response electrical charges which give rise to voltage, hence production of useful energy. The dimensions of the central piezoelectrical mass are length $300\ \mu\text{m}$, width $280\ \mu\text{m}$ and a thickness of $4\ \mu\text{m}$. The central mass vibrates under the action of force or harmonics to produce the required energy and also feasible for measuring vibrations present in the structure as a function of the voltage vs displacement.

2.1.3 Bimorph Temperature Sensor

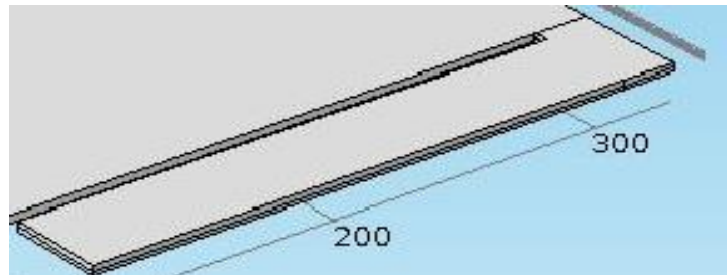


Figure 2.4a: Bimorph Temperature Sensor

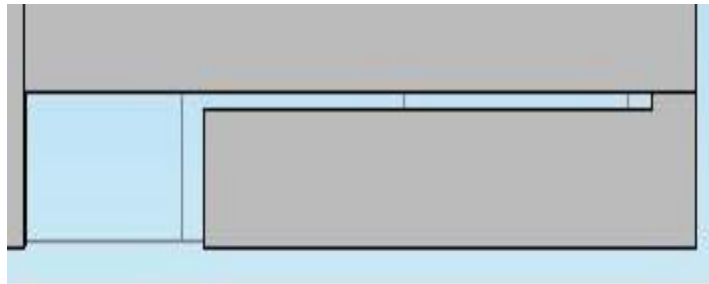


Figure 2.4b: Top View of Bimorph Temperature Sensor

As the name depicts bimorph is a bimetallic strip that deflects in the direction of material with higher thermal coefficient. The two metals may a combination of two metal strips (conductors) or one conductor and one semi-conductor. In the above figure 2.4a 3D view of the bimorph is shown with a top view in figure 2.4b. The bimorph consists of two metal layers of which upper layer is of aluminum and lower one is silver (argentum). As there is a rise in the temperature the bimorph starts displacing i.e. deflecting and shows a displacement by bending towards aluminum. The size of one side bimorph is $220\ \mu\text{m}$ length, $35\ \mu\text{m}$ width and $4\ \mu\text{m}$ thickness, with same dimensions for the other side too. For observing this effect joule heating and thermal expansion module is explored in detail and the simulation and results are discussed in the chapters to follow.

2.2 Mathematical Modeling

Mathematical Modeling of displacement for the above energy harvester is calculated. The beam is divided into two portions for the modeling purposes. 1st part is the anchor part and the 2nd is the piezoelectric part or the main mass, when load is applied at the boundary of the piezoelectric mass. The beam sectioning is presented in the figure 2.5 below.

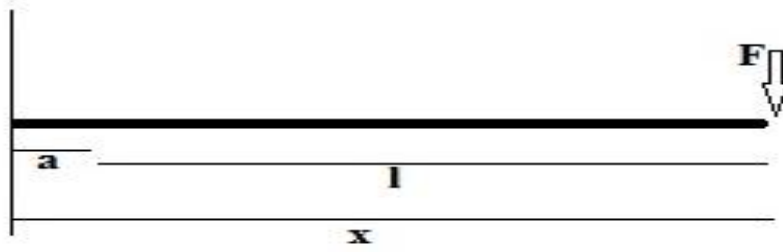


Figure 2.5: Piezoelectric beam model

The beam is fixed at one end and free from the other where a is the length of anchor, l is the length of piezoelectric and F is the load applied. Equation governing the displacement of the above beam is as under

$$EIy''' = F \quad \text{Equation 2.1}$$

Where E is the modulus of Elasticity, I is the moment of inertia, y is the displacement and F is the load applied. The boundary conditions are

$$y(0) = 0$$

$$y'(0) = 0$$

$$y''(l) = 0$$

Now integrating the above equation 2.1 gives

$$EIy'' = Fx + c \quad \text{Equation 2.2}$$

$$y = \frac{Fx^2(x-3l)}{6EI} \quad \text{Equation 2.3}$$

$$EIy = \frac{Fx^3}{6} - \frac{(Fl)x^2}{2} + c_2x + c_3 \quad \text{Equation 2.4}$$

c_2, c_3 are the constants and x is the length along the axis. Further solving the above equations for y (displacement) i.e. equation 2.2 by applying the boundary conditions gives

$$E_1I_1y'_a = \frac{Fa^2}{2} - Fla \quad \text{Equation 2.5}$$

$$E_1 I_1 y_a = \frac{F a^2}{6} (a - 3l) \quad (0 < x < a) \quad \text{Equation 2.6}$$

$$E_2 I_2 y'_a = \frac{F a^2}{2} - F l a + c_2 \quad \text{Equation 2.7}$$

$$E_2 I_2 y_a = \frac{F a^3}{6} - \frac{F l a^2}{2} + c_2 a + c_3 \quad (a < x < l) \quad \text{Equation 2.8}$$

Values of c_2 and c_3 can be calculated by using the above equations which comes to be

$$c_2 = \left(\frac{\frac{F a^2}{2} - F l a}{E_1 I_1} \right) E_2 I_2 - \frac{F a^2}{2} + F l a \quad \text{Equation 2.9}$$

$$c_3 = \left(\frac{\frac{F a^2}{6} (a - 3l)}{E_1 I_1} \right) E_2 I_2 - \frac{F a^3}{6} + \frac{F l a^2}{2} - c_2 a \quad \text{Equation 2.10}$$

The maximum displacement of the beam is calculated by the equation 2.11 which is the result of the above equations

$$y_{max} = y(l) = -\frac{F l^3}{2 E_2 I_2} + \frac{c_2 l + c_3}{E_2 I_2} \quad \text{Equation 2.11}$$

Replacing the values in of $E_1, I_1, E_2, I_2, F, l, c_3$ and c_2 in the equation the displacement is calculated.

$$y_{max} = y(l) = -4.3219 e^{-9} m$$

Graphical result of calculated displacement as solved in MATLAB using the above mathematical model in comparison with the simulated displacement of the device is shown in chapter 4 (graph 4.1, page 48).

2.3 Properties of Material Used in the design

A total of 4 materials are used in the design namely Silicon, Lead Zirconate Titanate (PZT-5A), Aluminum and Argentum (Silver). For the material used the properties are tabulated for the respective material.

Silicon that is being used in anchor has the following properties as per FEM software (COMSOL Multiphysics) like Young's Modulus, Poisson's ratio, Density, relative permittivity etc as tabulated below in table 1

Sr. No	Property	Value	Unit
1.	Young's Modulus (E)	170e9[Pa]	Pa
2.	Poisson's Ratio (nu)	0.28	1
3.	Density (rho)	2329[kg/m ³]	kg/m ³
4.	Relative Permittivity (epsilon)	11.7	1
5.	Heat Capacity (Cp)	700[J/(kg*K)]	J/(kg*K)
6.	Co-efficient of thermal expansion (alpha)	6e-6[1/K]	1/K

Table 2.1: Silicon material properties

For Piezoelectric material Lead Zirconate Titanate (PZT5A) is used. As it is the make part of the design and the most important one following are some of the properties tabulated below found in literature and COMSOL Multiphysics material library.

Sr. No.	Property	Value	Unit
1.	Young's Modulus (E)	63e9[Pa]	Pa
2.	Density (rho)	7750[kg/m ³]	kg/m ³
3.	Relative Permittivity (epsilon)	{1730, 1730, 1700}	1
4.	Coupling Co-efficient (eES)	0.66	1
5.	Dielectric Constant, Relative	1700	1
6.	Strain Co-efficient	3.6e-10 m/V	m/V
7.	Voltage Co-efficient	0.025V*m/N	V*m/N

Table 2.2: PZT 5A material properties

For Aluminum important material properties used are Young's Modulus 70.0e9[Pa], Density 2700[kg/m³], Poisson's ratio 0.35, Co-efficient of thermal expansion 23.1e-6[1/K] and heat capacity 904[J/(kg*K)] respectively.

For Silver important material properties used are Young's Modulus $83e9$ [Pa], Density 10500 [kg/m³], Poisson's ratio 0.37 , Co-efficient of thermal expansion $18.9e-6$ [1/K] and heat capacity 235 [J/(kg*K)] respectively.

CHAPTER 3: SIMULATIONS

This chapter includes the simulations that are performed not only on the energy harvester described in the last chapter but also of all the designs explored before reaching the final design and also discusses the reasons of the rejection of the designs with the respective design under consideration. Comsol Multiphysics (FEM software) is used for the designing, analysis and simulation purposes.

3.1 Energy Harvester Design 1(electrostatic)

The first design for the energy harvester is shown in figure 3.1 that was based on making use of structural vibrations. The design consists of the central vibrating mass and four serpentine springs used to support the mass and acting as anchor. When a mechanical force is applied at the mass, the mass starts vibrating in the direction of force.

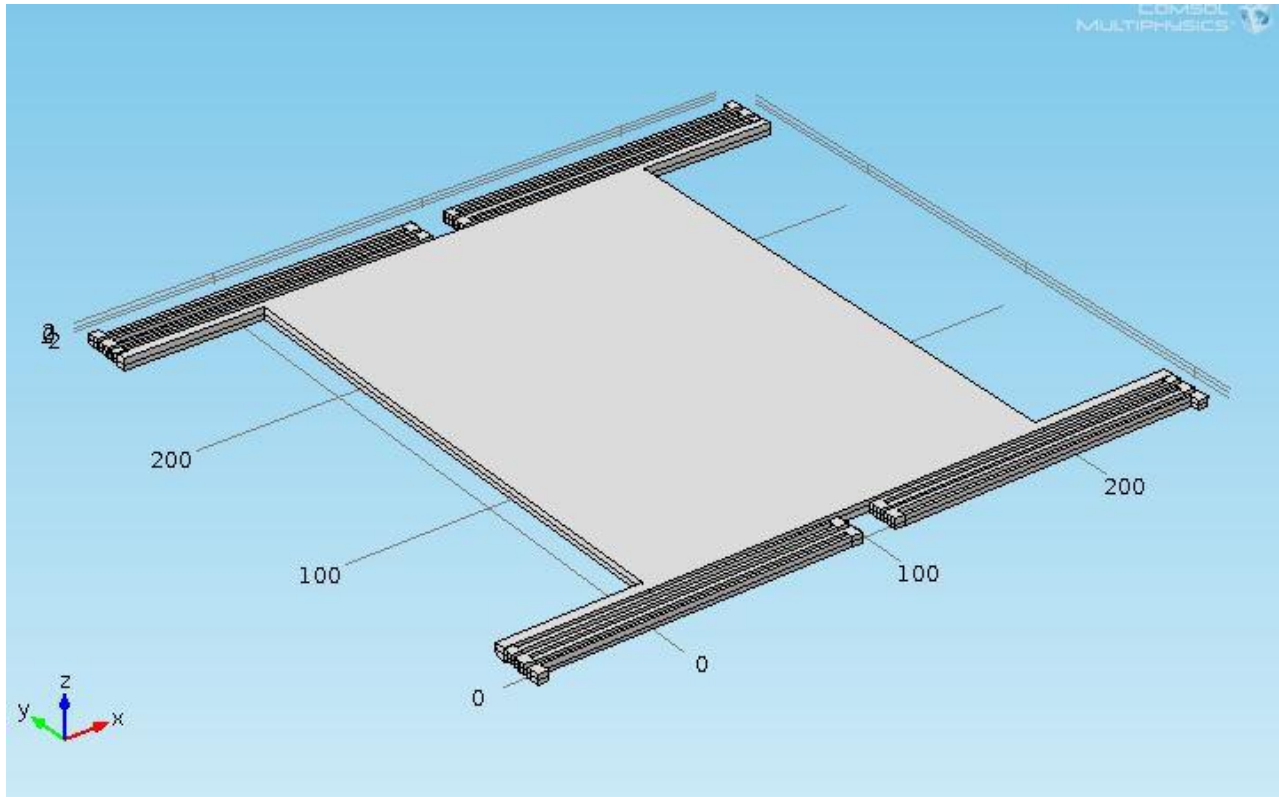


Figure 3.1: Vibration based Energy Harvester

3.1.1 Simulation results of Design 1

The energy harvester was observed in detail but the required results were not achieved due to some critical design parameters not taken into account. The serpentine springs were too flexible and had very low stiffness due to which they cannot withstand cyclic loads. The harvester is $360\mu\text{m} \times 360\mu\text{m}$ with a thickness of $8\mu\text{m}$. Some of the results are as under

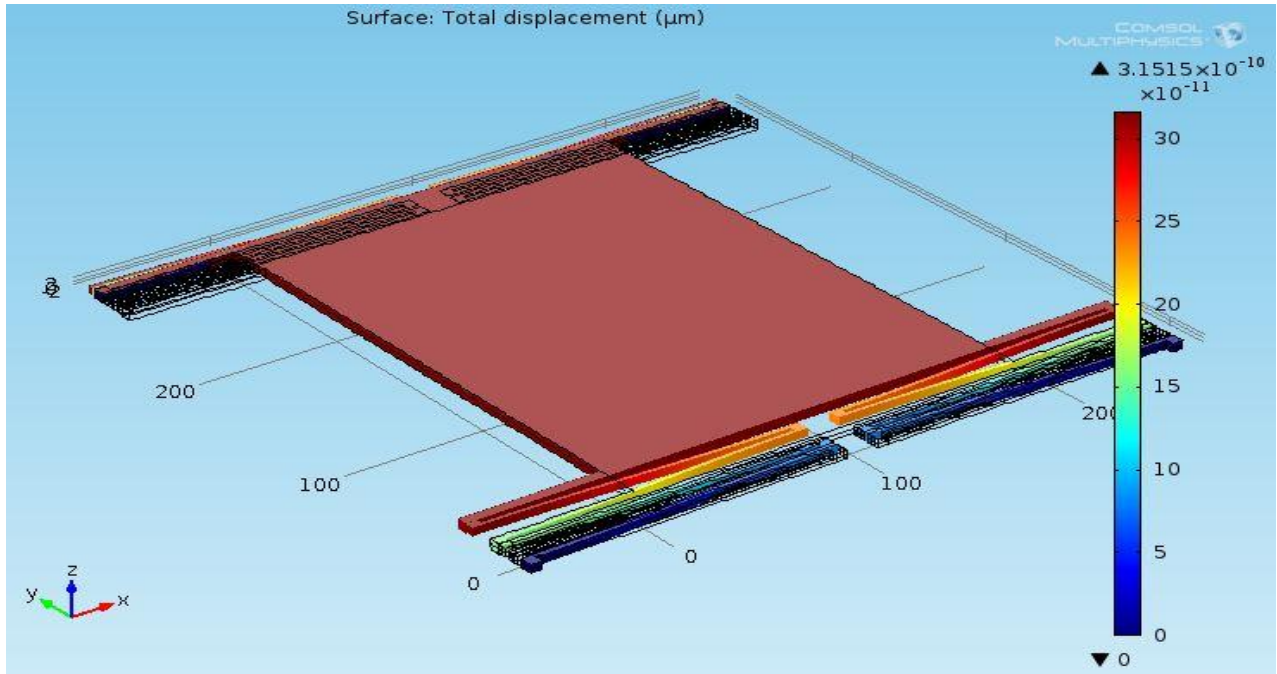


Figure 3.1.1: Displacement results of the EH when subjected to small loads

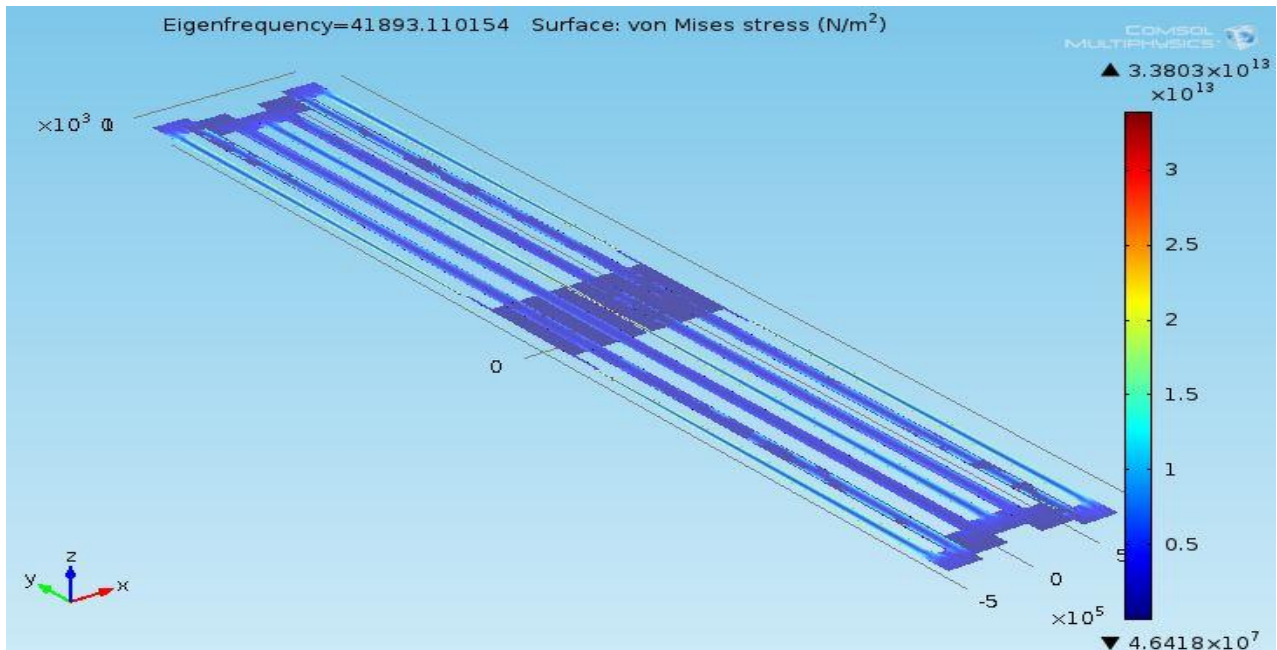


Figure 3.1.2: Stress values of the EH subjected to small mechanical loading

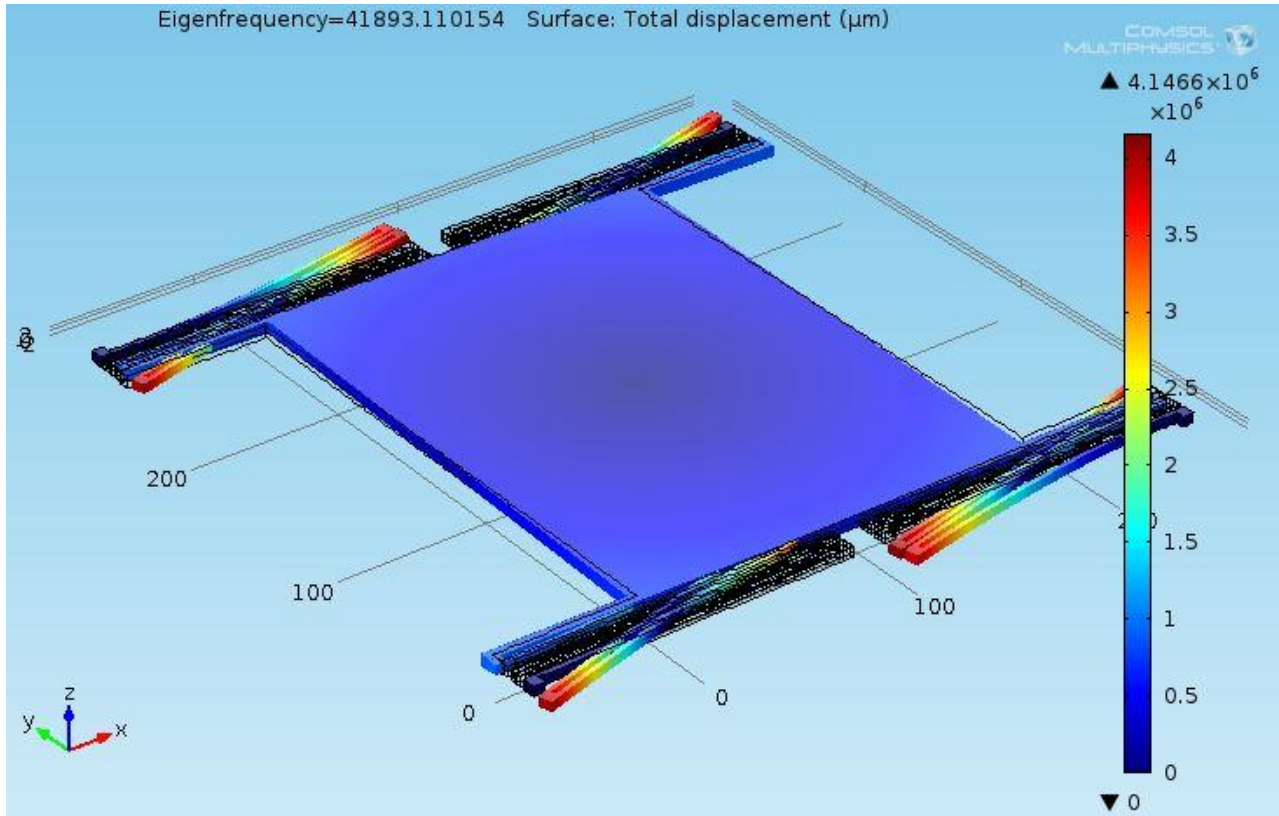


Figure 3.1.3: Frequency Analysis of the energy harvester

The low stiffness of serpentine springs is quite clear from the simulations and pictorial view shown in figures 3.1.1, 3.1.2 and 3.1.3.

3.2 Capacitive Energy Harvester Design (Design 2)

Capacitive energy harvester as shown in figure 3.2 is improvement in design 1. The four serpentine springs are replaced by 2 springs being bigger in size and stiffer than the previous one. Anchor being added around the whole periphery of the harvester and springs being attached to the anchor along with comb fingers. The comb fingers act as capacitor, due to the movement of the mass the gap between the fingers change and hence producing a capacitive effect as they are acting as parallel plate capacitors. The serpentine springs are designed to be made of two different metals i.e. aluminum and poly-silicon in order to behave like bimorphs so that they can detect the changes in the temperature. A detailed analysis of design is carried out involving static analysis, frequency analysis, time dependent analysis and dynamic analysis. The results of the simulations are not according to the expectations and the device performed low par. The design was rejected due to very low capacitance value being produced in the process and complexity of increasing the comb drives limits the design.

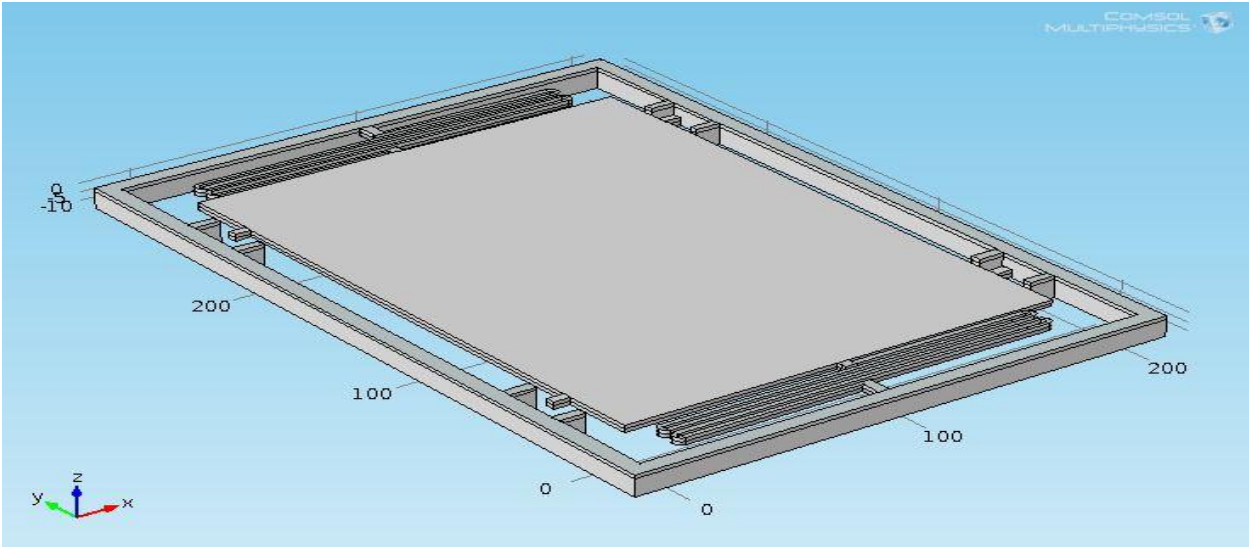


Figure 3.2: Capacitive Energy Harvester Design

3.2.1 Simulation Results of capacitive energy harvester

A detailed analysis of the design is carried out but the device failed to produce the expected results. The overall size of harvester is $360\mu\text{m} \times 230\mu\text{m}$ and a thickness of $12\mu\text{m}$ at anchor and comb drive whereas the thickness of serpentine springs and mass is $4\mu\text{m}$.

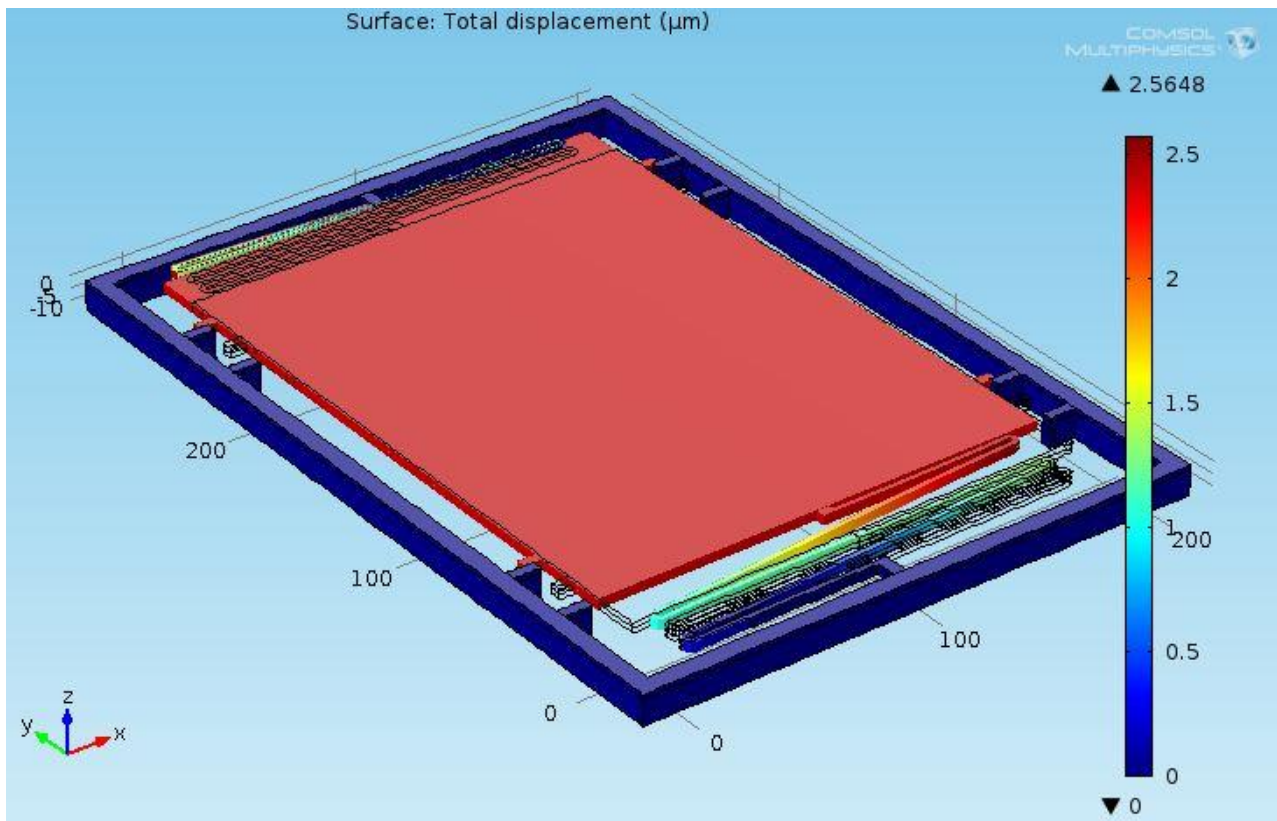


Figure 3.2.1: Static analysis, Displacement of mass

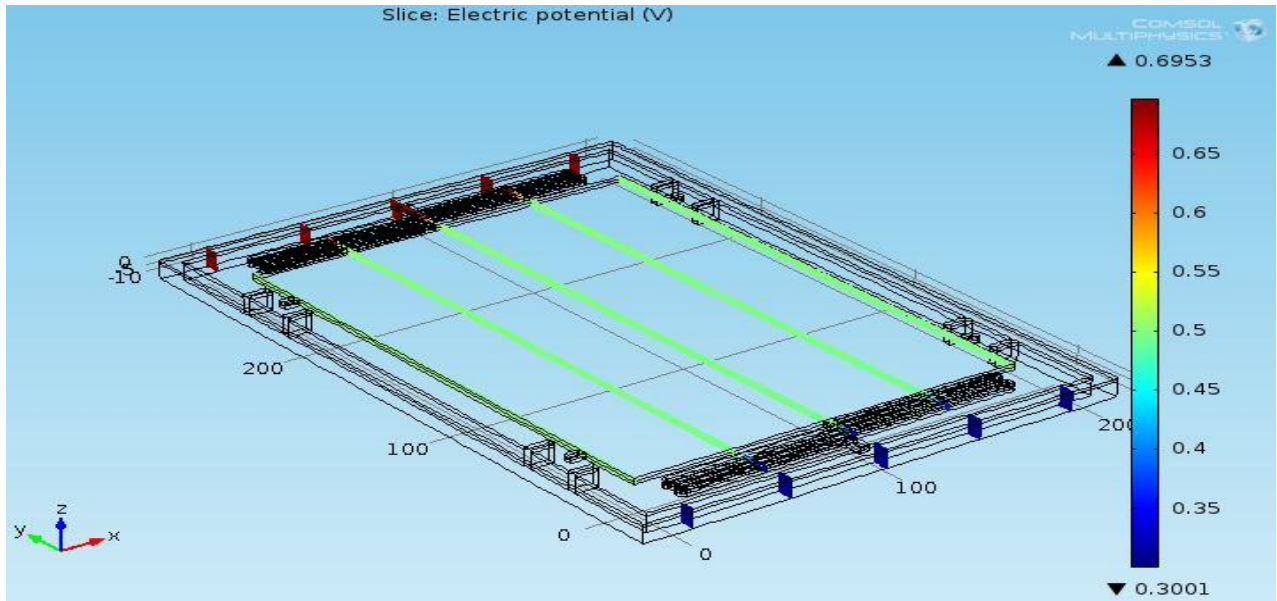


Figure 3.2.2: Static Analysis, Produced Voltage

After the static analysis, frequency analysis is carried out. Four out of six modes of modal analysis are represented as under

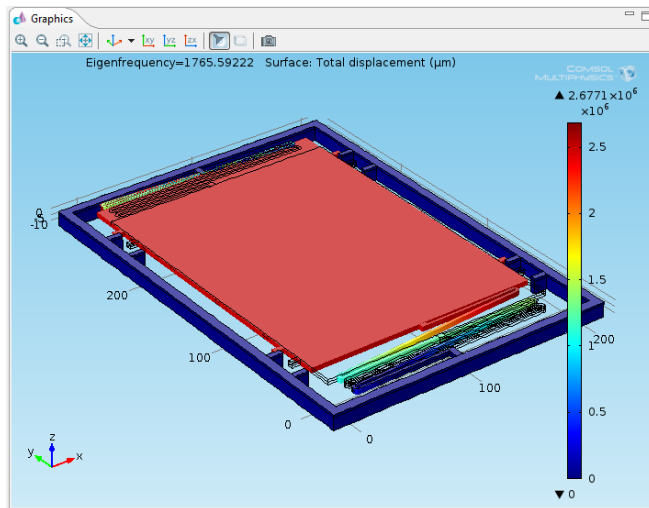


Figure 3.2.3: 1st mode frequency

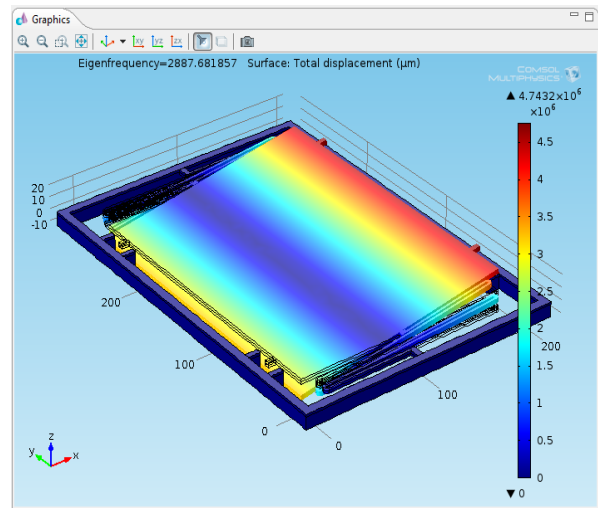


Figure 3.2.4: 2nd mode frequency

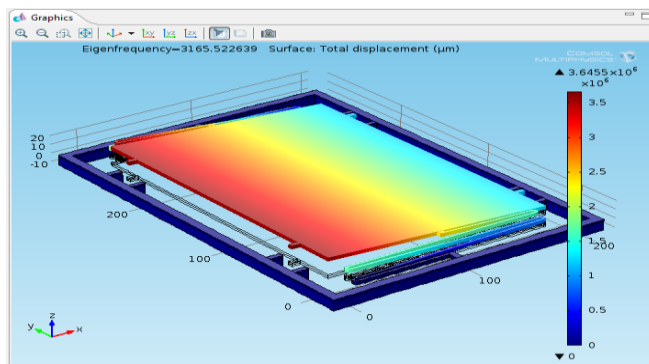


Figure 3.2.5: 3rd mode frequency

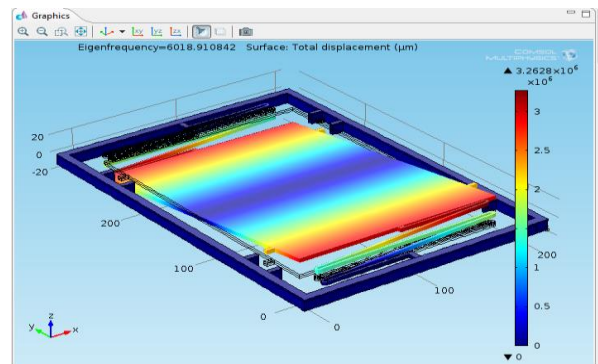


Figure 3.2.6: 4th mode frequency

Next temperature analysis is represented. The effect of temperature on serpentine springs is studied and effectiveness of the said is judged resulting into a rejection of the design.

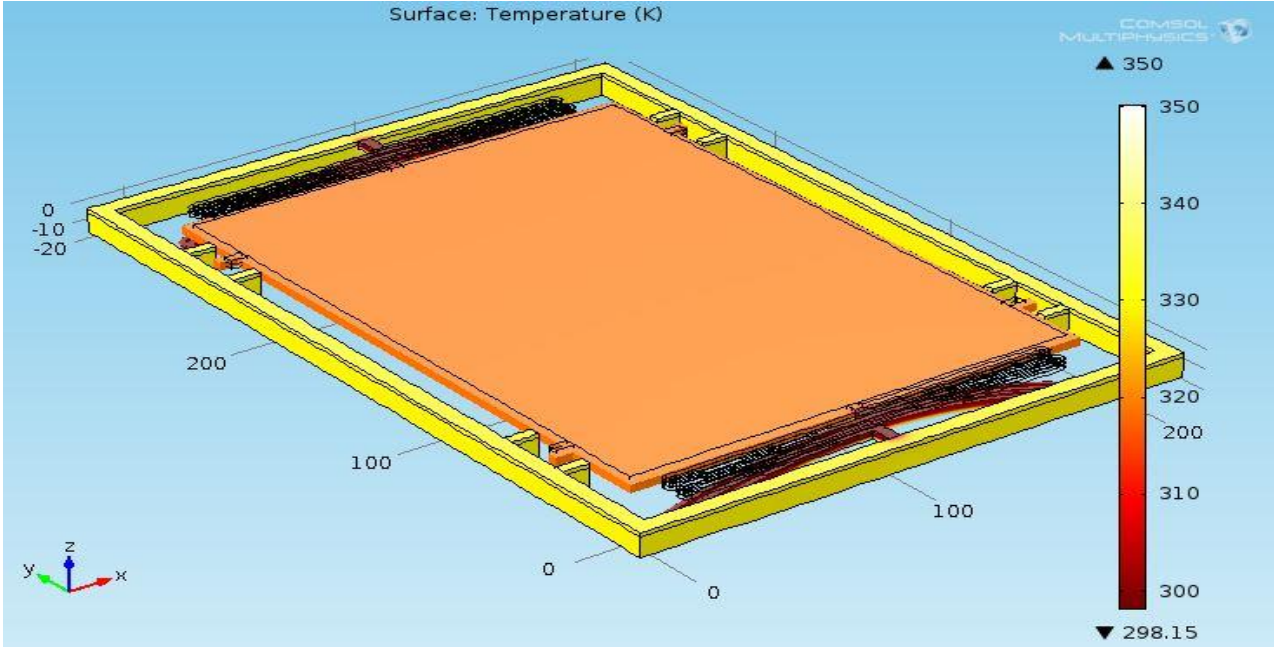


Figure 3.2.7: Temperature effect on the device especially on springs

Further the capacitance graph is resented in figure 3.2.8 showing very low and unacceptable capacitance

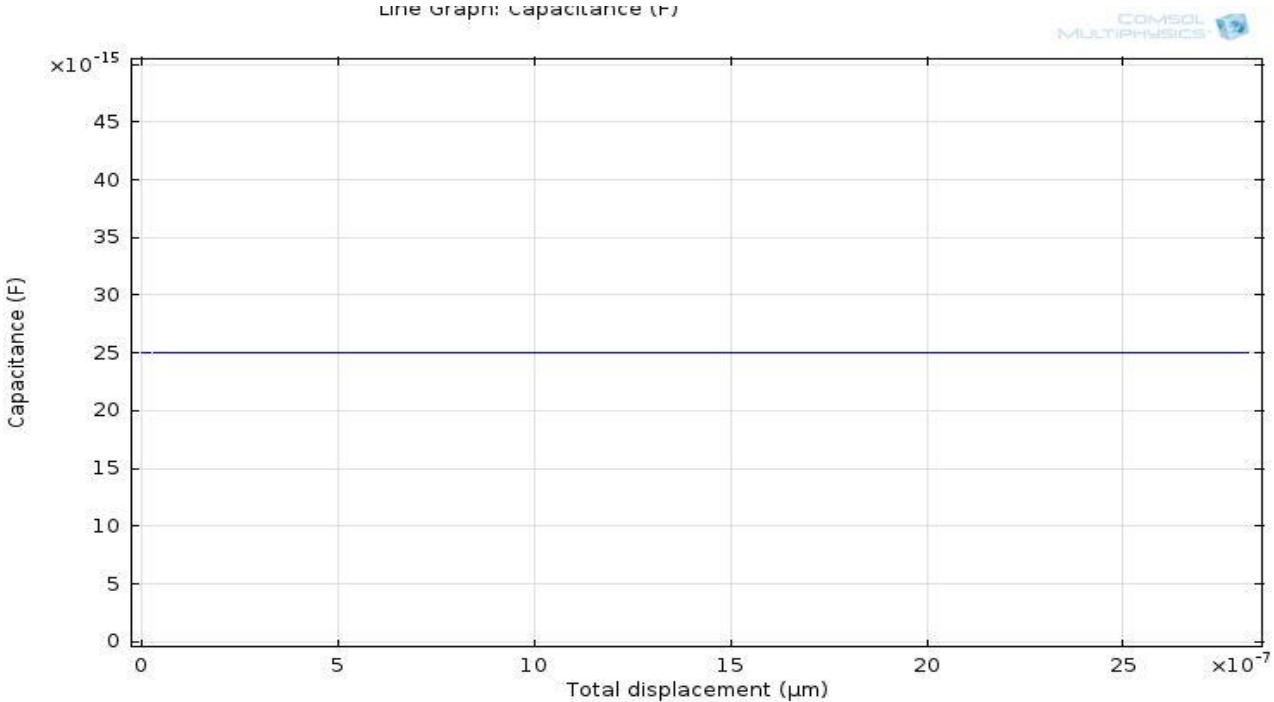


Figure 3.2.8: Capacitance results of capacitive energy harvester

3.3 Bimorph Piezoelectric Energy Harvester (Design 3)

Because of the advantages of piezoelectric energy harvesters especially in respect of better outputs, piezoelectric designs are investigated. A bimorph piezoelectric energy harvester is presented in figure 3.4 which consists of an anchor to which five bimorph piezoelectric cantilever beams are connected. Bimorph idea is again to measure temperature changes aside from energy harvesting utilizing the vibrations of the structures. The dimension of energy harvester is $330\mu\text{m} \times 360\mu\text{m}$.

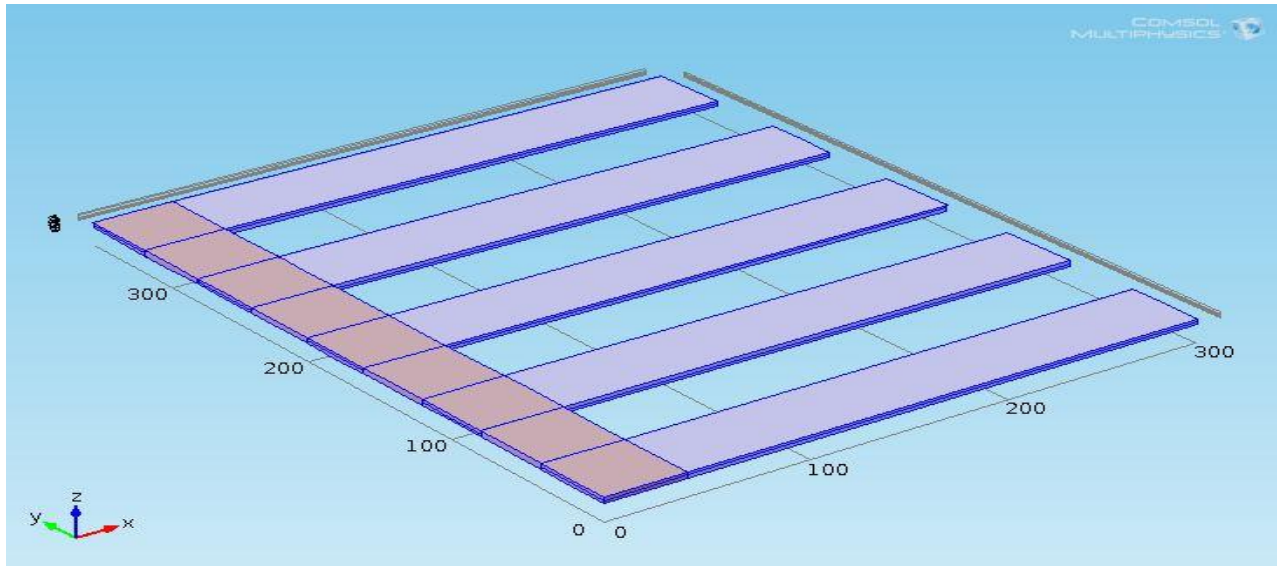


Figure 3.3: Bimorph piezoelectric energy harvester

3.3.1 Simulation results of the bimorph energy harvester

Some of the selected results are presented in the figures below. Due to the design limitation of measurement of temperature and fabrication problems the techniques is not further investigated as it also becomes obvious from the results to follow.

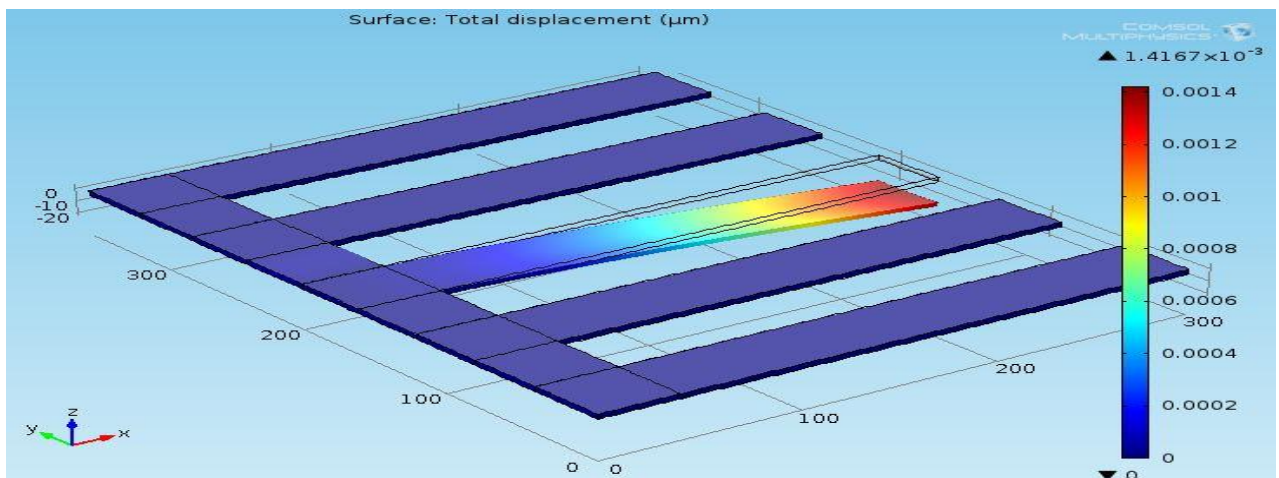


Figure 3.3.1: Static analysis, displacement of bimorph piezoelectric cantilevers

Frequency analysis is presented in figure 3.3.2 and the corresponding voltage output in figure 3.3.3. The results show complex and imaginary values of eigen frequency.

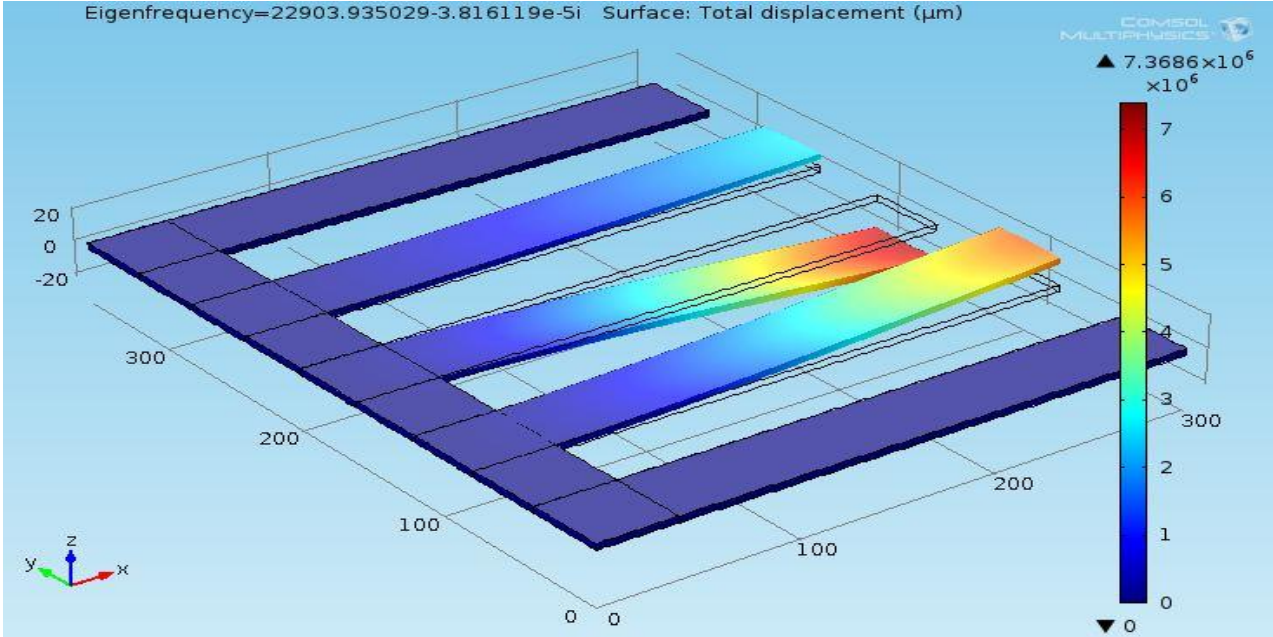


Figure 3.3.2: Frequency Analysis of bimorph piezoelectric energy harvester

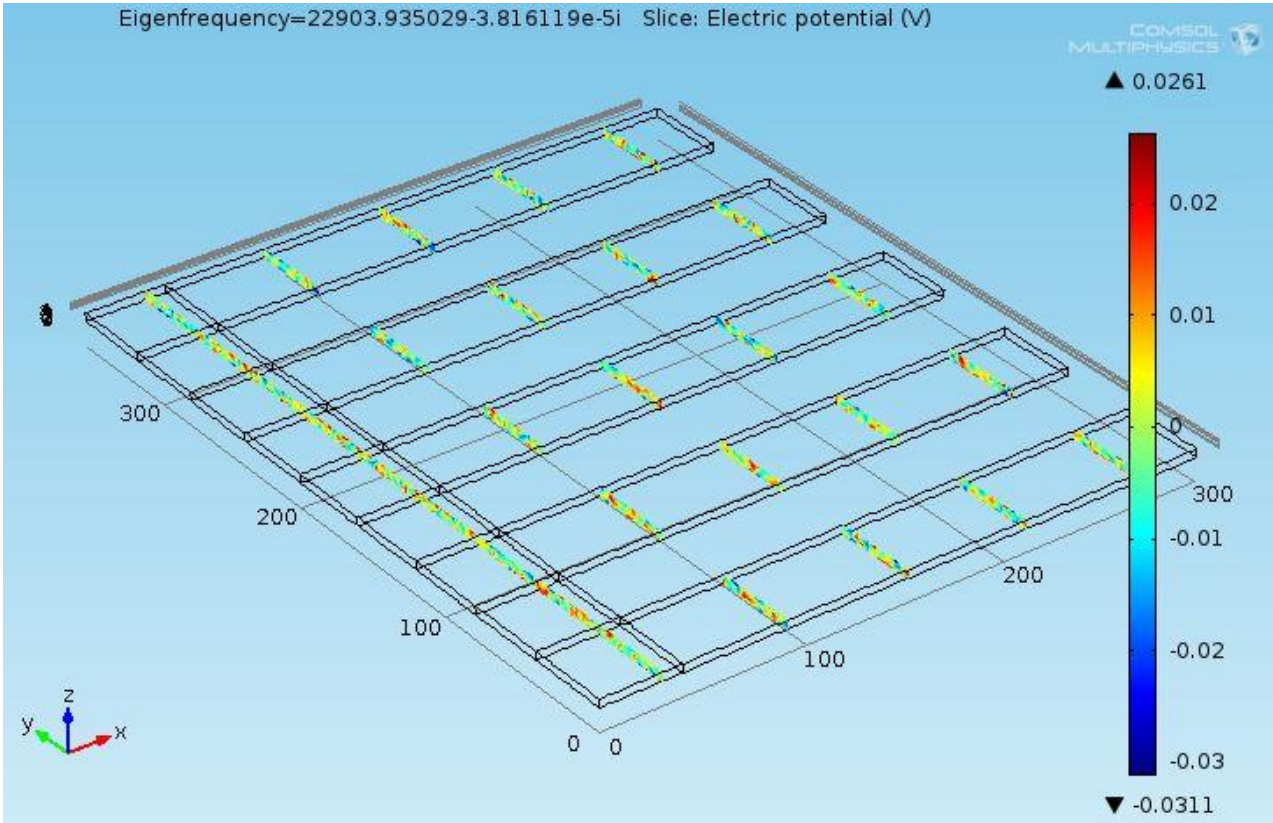


Figure 3.3.3: Voltage output of the EH at resonance frequency

3.4 Piezoelectric Energy Harvester with Temperature Sensor (Bimorph)

Piezoelectric energy harvester is designed with an additional capability of temperature sensing based on bimorph concept i.e. as the temperature increases the bimorph starts to deflect/ bend in the direction of the material having low coefficient of thermal expansion, the displacement shows the increase in the temperature. Figure 3.4 shows a piezoelectric energy harvester having an anchor to which a piezoelectric energy scavenging portion is attached (cantilevered) and bimorph portion is further attached (cantilevered) with the energy harvesting part. The size of the whole device is $360\mu\text{m} \times 330\mu\text{m}$ (length x width) with a thickness of $4\mu\text{m}$.

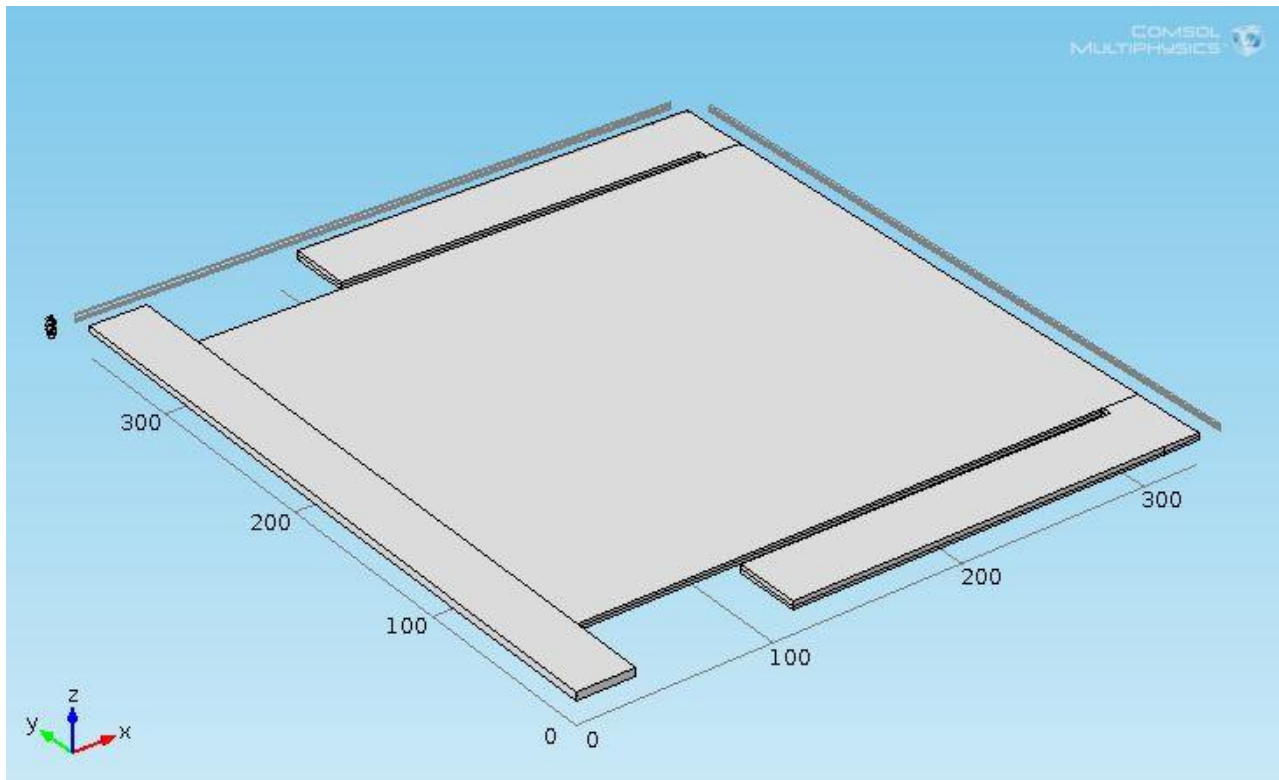


Figure 3.4: Cantilevered based Single layer Piezoelectric Energy Harvester along with Temperature Measuring Bimorph

The piezoelectric energy harvester shown in figure 3.4 consists of three parts as already described in detail in chapter 2. The cantilevered piezoelectric energy scavenger portion is single layered i.e. made up of only one layer of Lead Zirconate Titanate (PZT 5A) where as the bimorph portion consists of silver and aluminum being the lower and upper surfaces respectively. The anchor's material is Silicon to which the main portion is connected. Simulation results are discussed in the following sections.

3.4.1 Simulation Results, Static Analysis

Firstly the static analysis is presented in the figures below. The static analysis for three different thicknesses i.e. $T=8\mu\text{m}$, $T=6\mu\text{m}$ and $T=4\mu\text{m}$ is investigated (pictorial view of analysis for $T=4\mu\text{m}$ is shown in figure 3.4.1 and 3.4.2) and graphical representation is shown in figures 3.4.3 and 3.4.2.

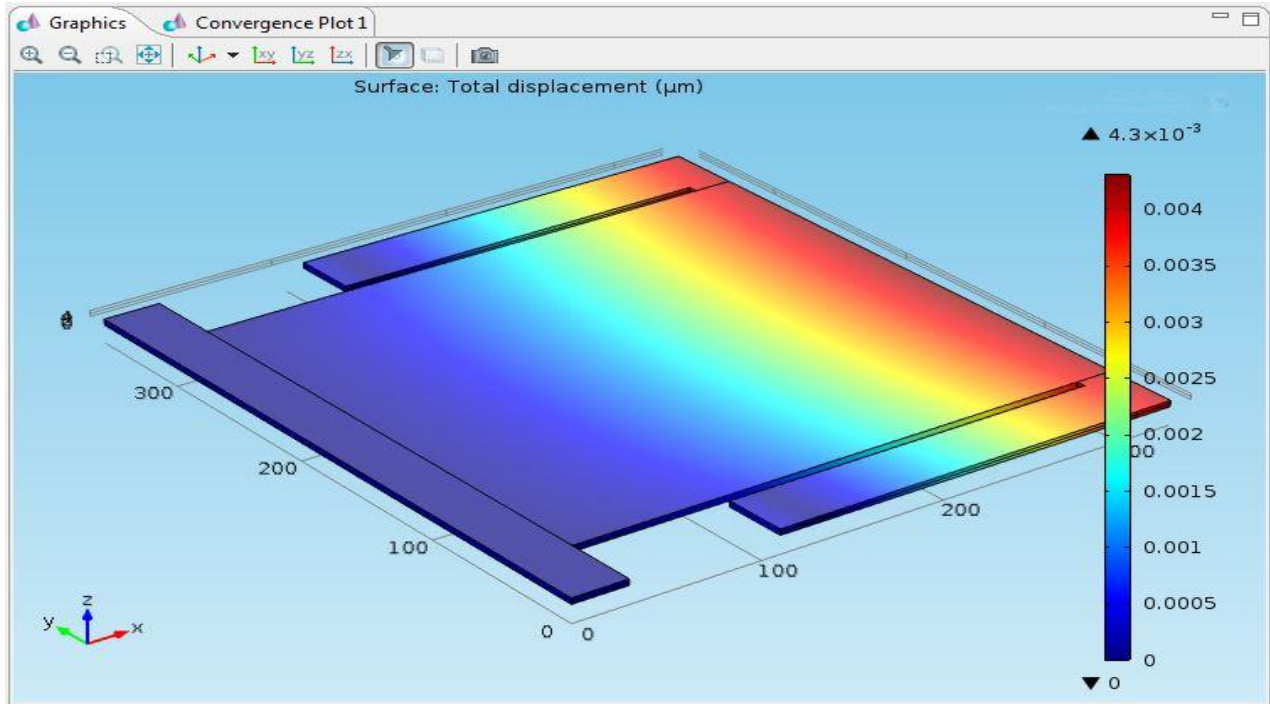


Figure 3.4.1: Static Analysis Displacement results for $T=4\mu\text{m}$

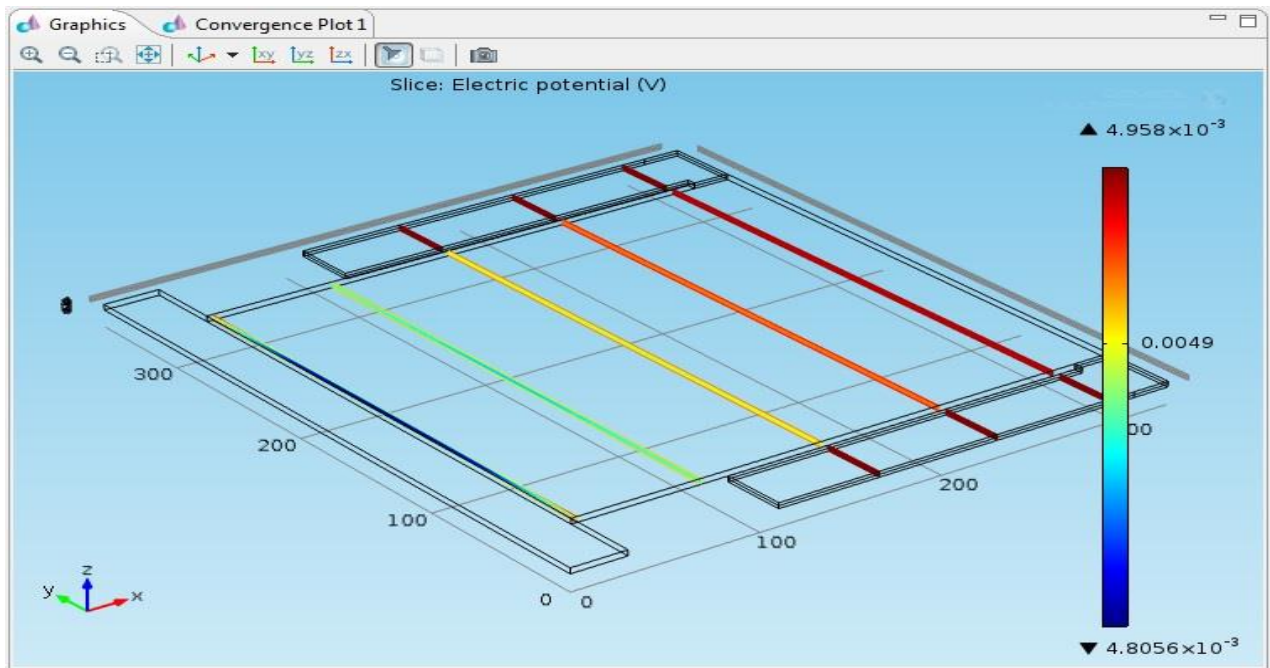


Figure 3.4.2: Static Analysis Voltage results for $T=4\mu\text{m}$

The results are further investigated for varying load and the best results are obtained for the minimum thickness used i.e. 4micron. Figures 3.5.3 and 3.5.4 represent the results for these thicknesses.

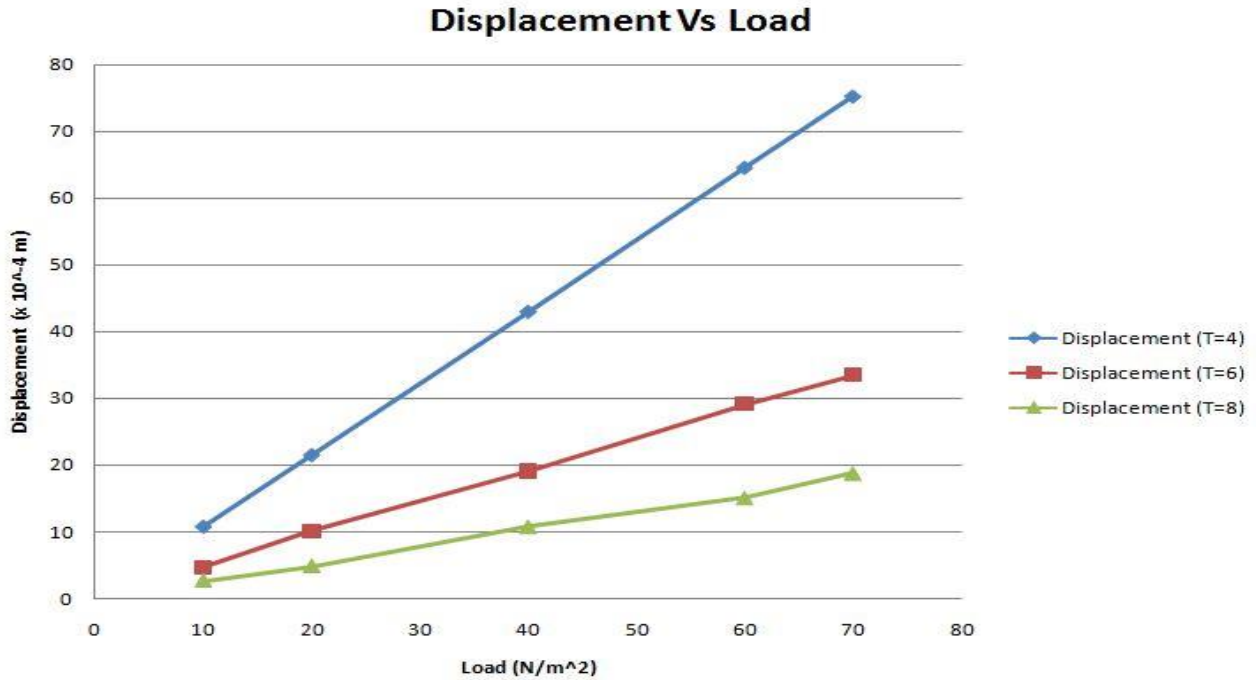


Figure 3.4.3: Graph showing displacement results of comparison for different thicknesses

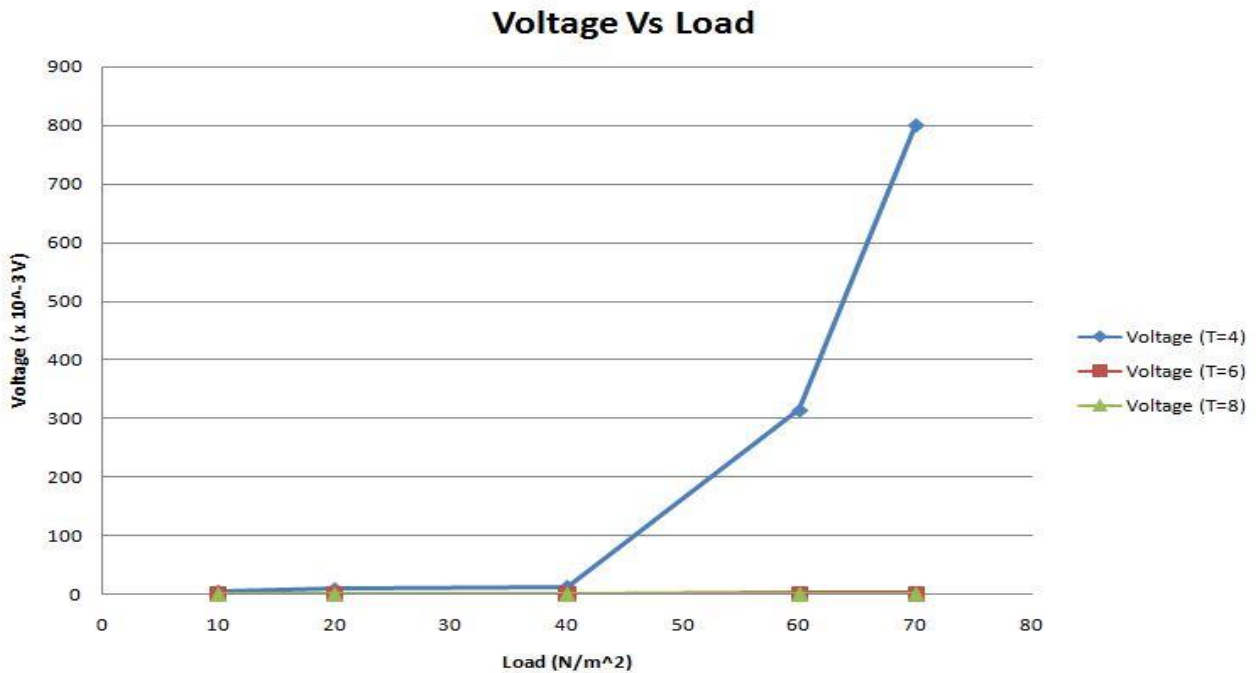


Figure 3.4.4: Graph showing voltage results of comparison for different thicknesses

The graphs represent the displacement and voltage results for thicknesses $T=8\mu\text{m}$, $T=6\mu\text{m}$ and $T=4\mu\text{m}$ at varying loads of 10N/m^2 , 40N/m^2 and 70N/m^2 showing that the best results were achieved for the thickness $T=4\mu\text{m}$.

3.4.2 Frequency Analysis

This device would generate output voltage as a result of vibrations therefore dynamic analysis is important. For that, frequency analysis is carried out and the design is investigated for higher frequencies. As the thickness decreases, the frequency decreases and vice versa. The application of the design requires frequency in the range of 15,000 to 18,000 Hz. The required results are successfully achieved by thickness of $4\mu\text{m}$. The frequency and respective voltage are represented in figures 3.4.5 and 3.4.6 respectively.

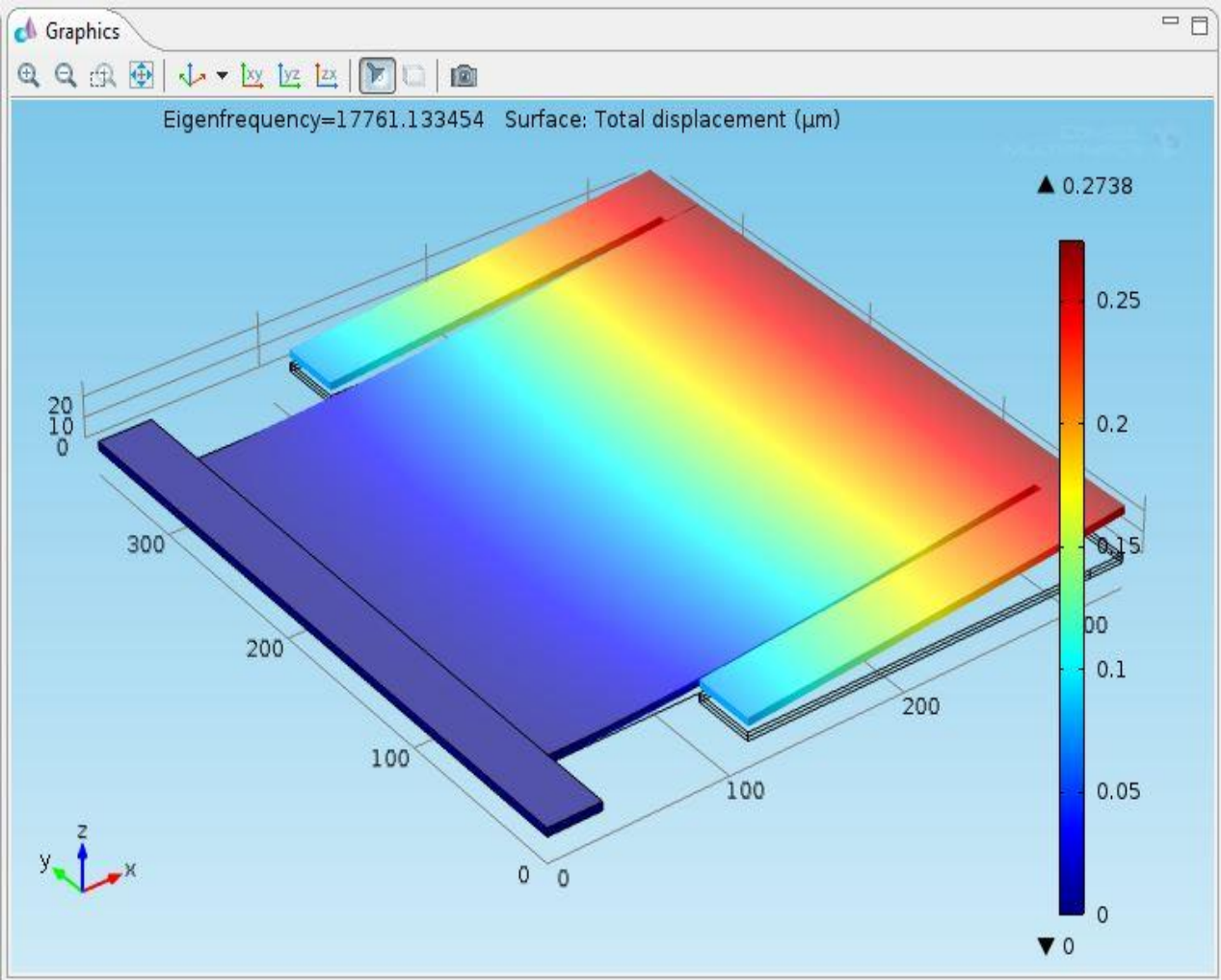


Figure 3.4.5: Frequency Analysis, Eigen Frequency results

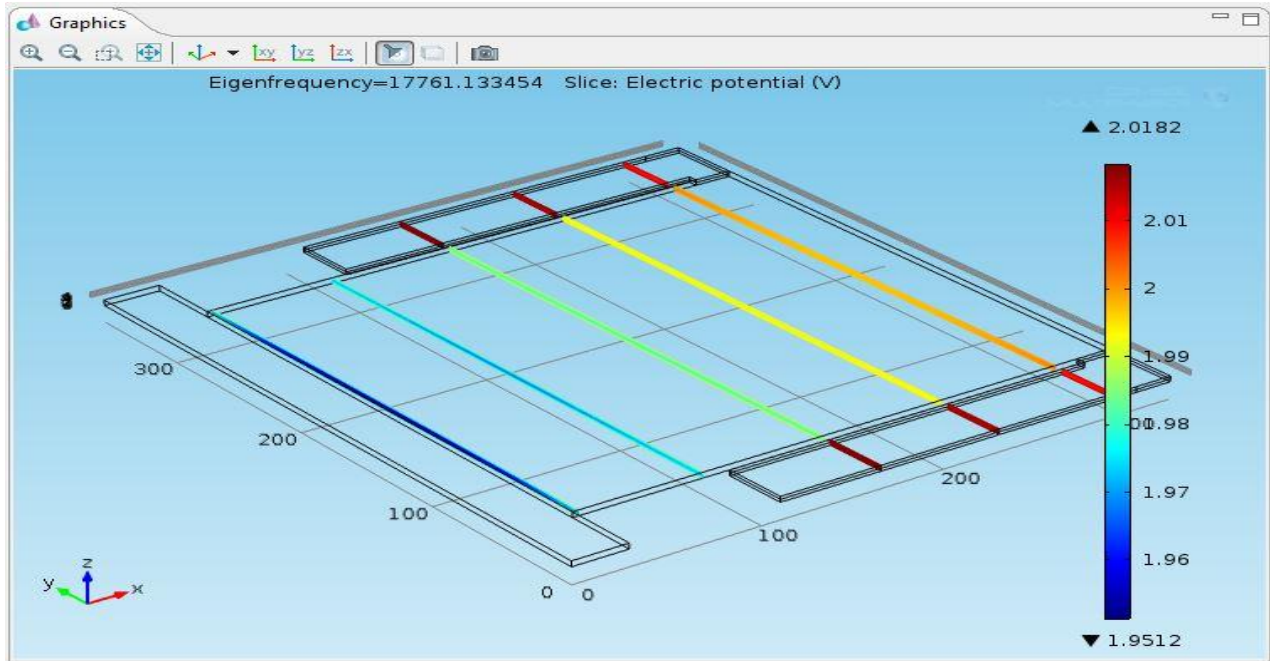


Figure 3.4.6: Frequency Analysis, Voltage results at frequency 17761 Hz

Next modal analysis is represented in figures 3.4.7, 3.4.8, 3.4.9, 3.4.10, 3.4.11 and 3.4.12 showing 1st, 2nd, 3rd, 4th, 5th and 6th modes of Eigen frequency respectively.

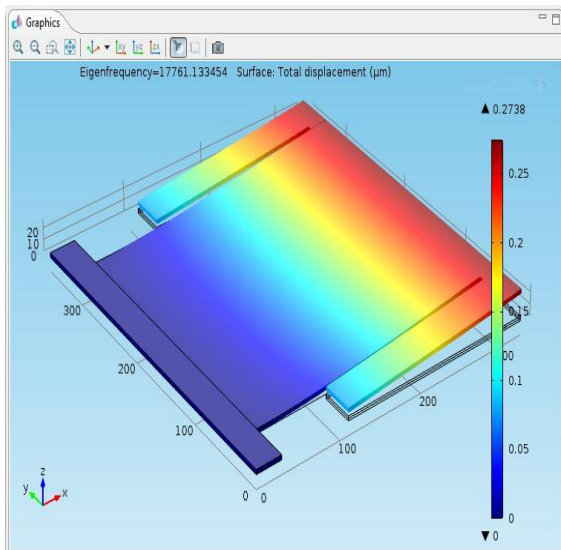


Figure 3.4.7: 1st Modal Frequency

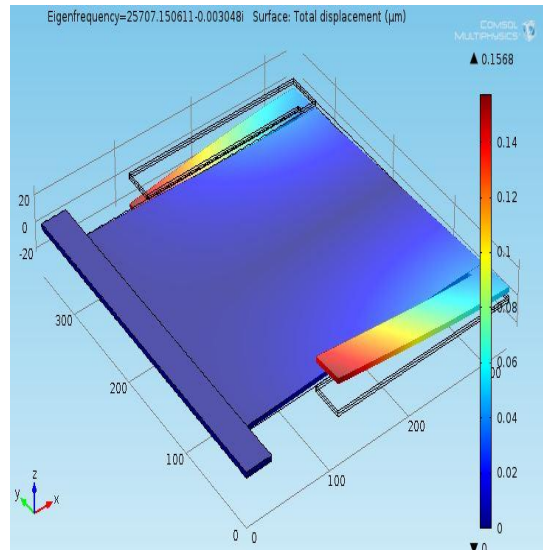


Figure 3.4.8: 2nd Modal Frequency

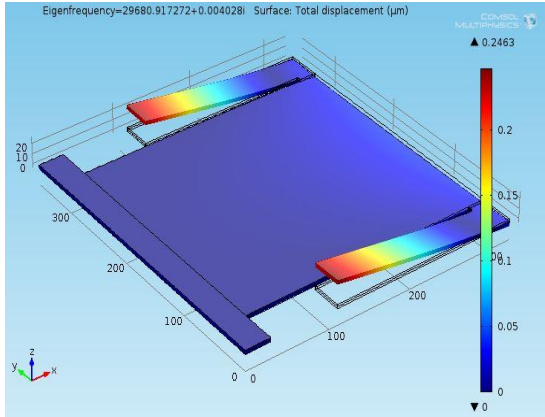


Figure 3.4.9: 3rd Modal Frequency

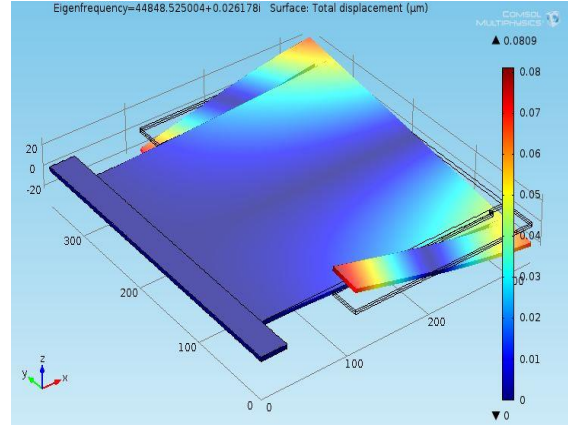


Figure 3.4.10: 4th Modal Frequency

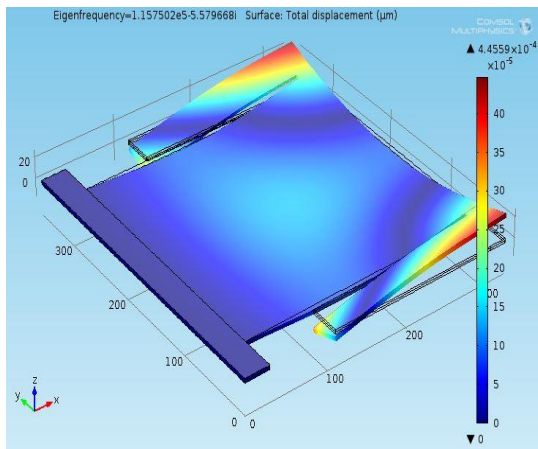


Figure 3.4.11: 5th Modal Frequency

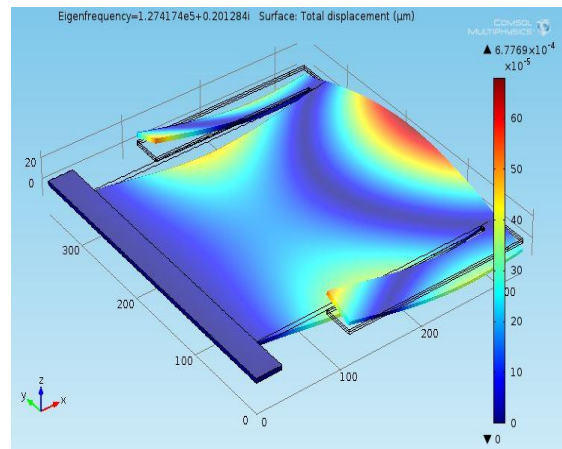


Figure 3.4.12: 6th Modal Frequency

3.5.3 Harmonic Sweep Simulations

Harmonic sweep is applied to determine the behavior of the piezoelectric cantilever at different frequencies. The values of harmonics are varied from 500 Hz to 17500 Hz and simulation is run to determine the displacement and voltage results. Applied harmonic frequency, displacement and voltage simulation results for harmonic frequency of 500Hz, 5500Hz, 13500Hz and 17500Hz are presented in figures 3.4.13, 3.4.14, 3.4.15, 3.4.16, 3.4.17 among which first three figures represent results for the harmonic frequency of 17500Hz and the rest two are the graphs showing the results of the harmonic sweep.

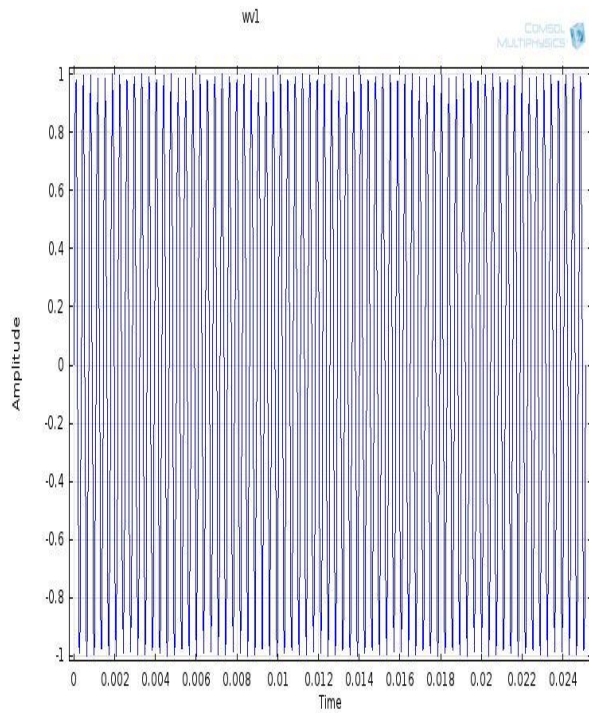


Figure 3.4.13: Applied Harmonic 17500Hz

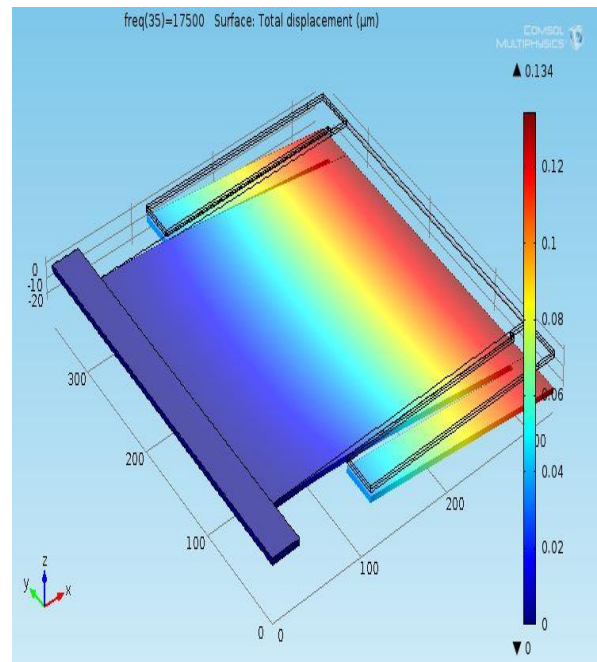


Figure 3.4.14: Displacement Results

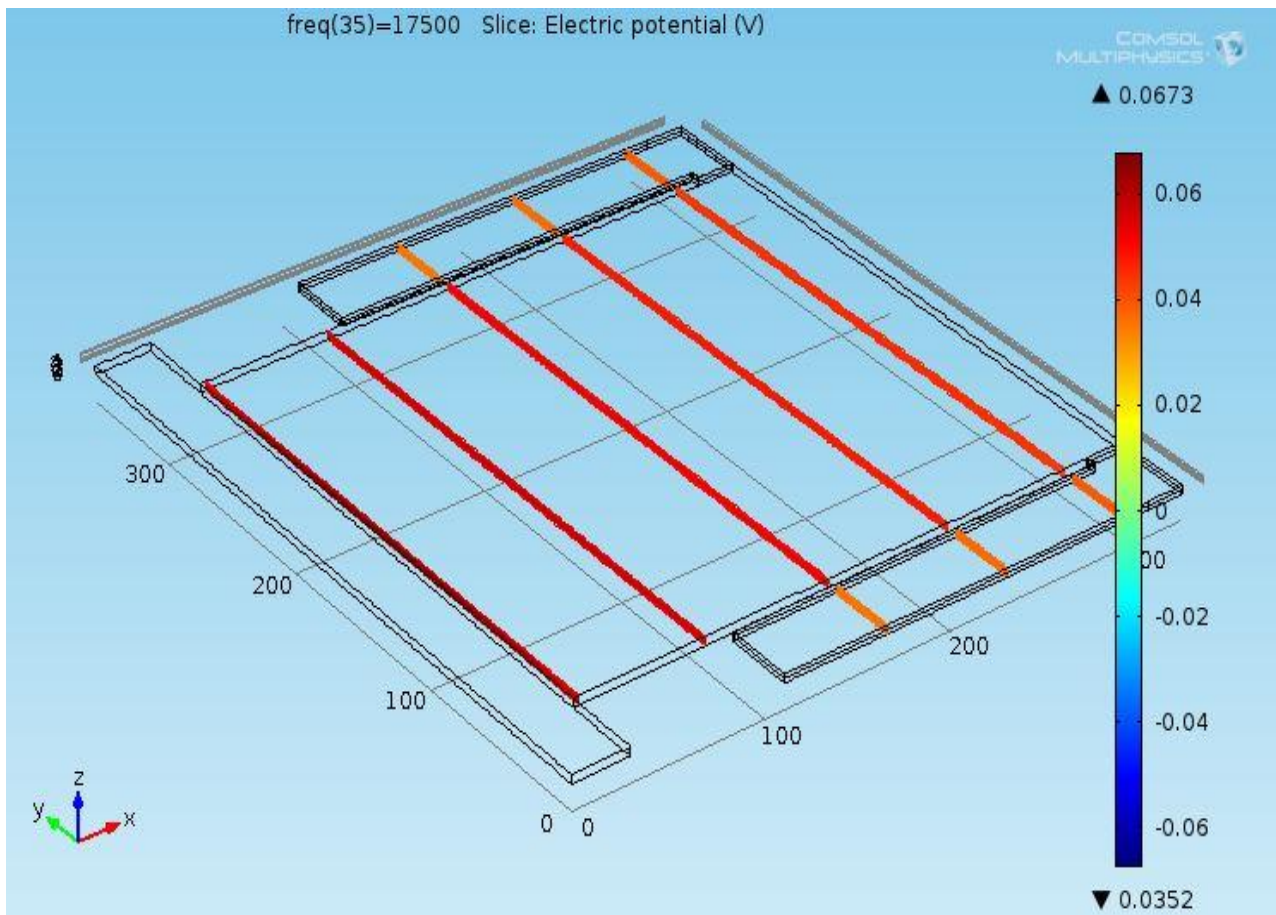


Figure 3.4.15: Voltage at Harmonic Frequency of 17500 Hz

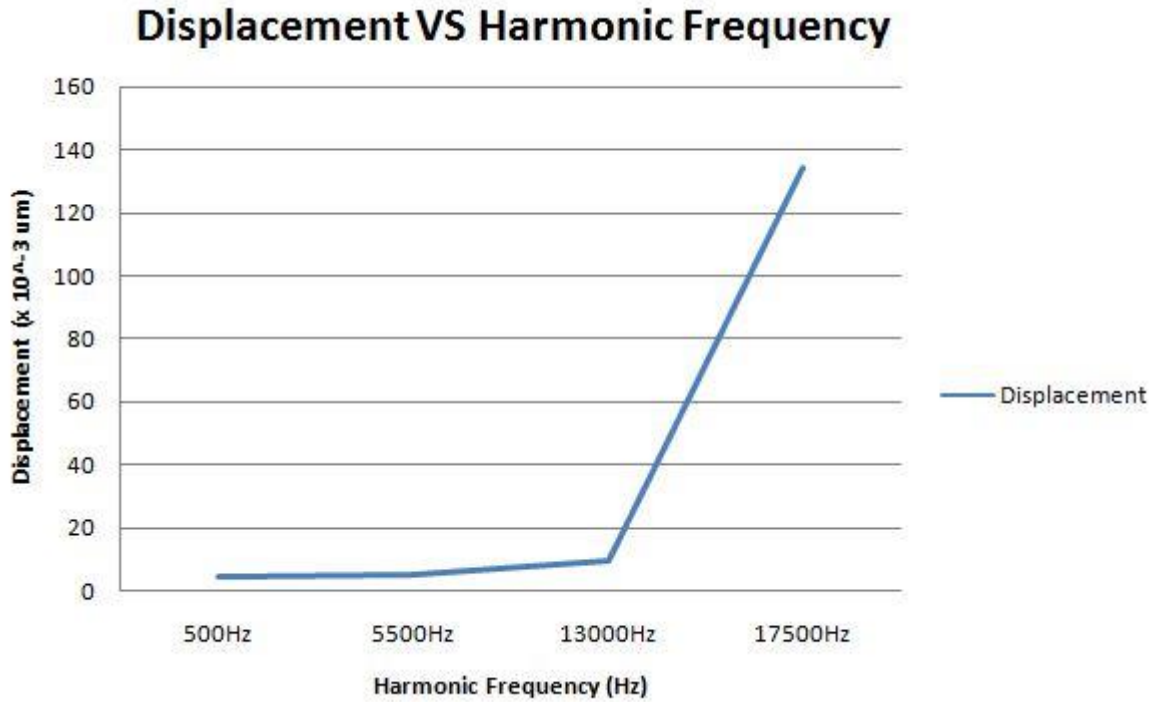


Figure3.4.16: Graph showing harmonic sweep results at different frequencies for displacement

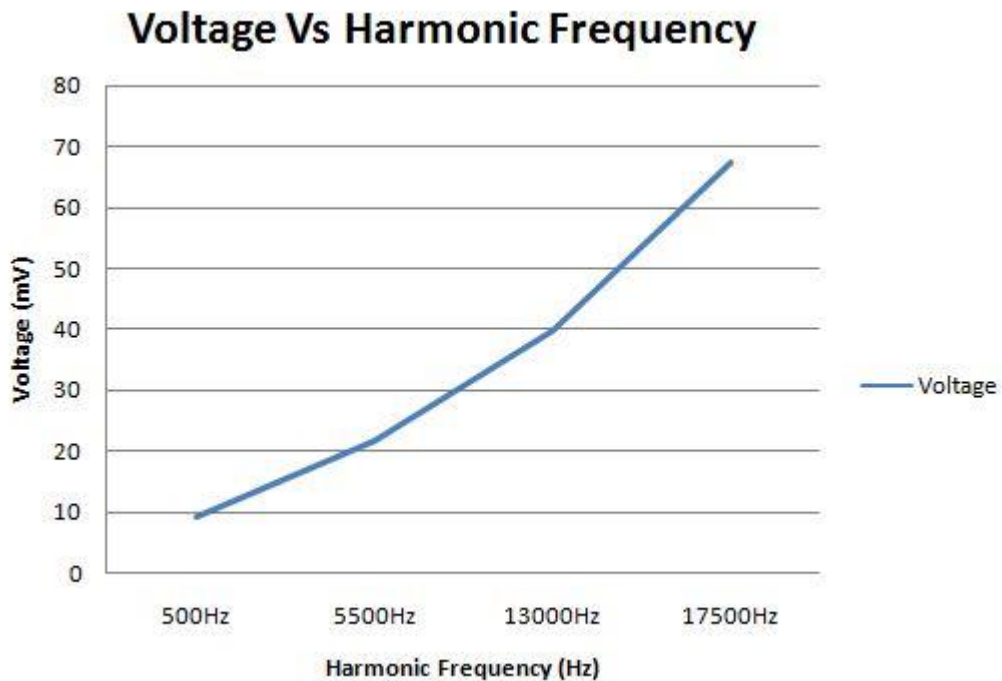


Figure3.4.17: Graph showing harmonic sweep results at different frequencies for voltage
 The graphs show that the results obtained at frequency 17500Hz are better in comparison with the other frequencies.

3.4.4 Bimorph Portion Simulation Results

The bimorph is designed to help in the temperature measurement of the structure in which the sensor is embedded. This portion provides an extra sensing to the device. Energy harvesters are just design to only scavenge the energy from the ambient sources; here the idea is to measure the temperature along with harvesting the energy from the source i.e. mechanical source or vibrations in this specific work. The bimorph portion consists of the two metal layers that are designed in such a way that as the temperature increases the bimetallic strip deflects/ bends in the direction of the metal having less coefficient of heat expansion. The upper layer is Aluminum whereas the lower layer is Silver. Simulation results are presented in the figures to follow. The temperature is raised from 295K to 339K and the device has a total displacement of $3\mu\text{m}$ (the bimorph portion) presented in the figures 3.4.18 to 3.4.23.

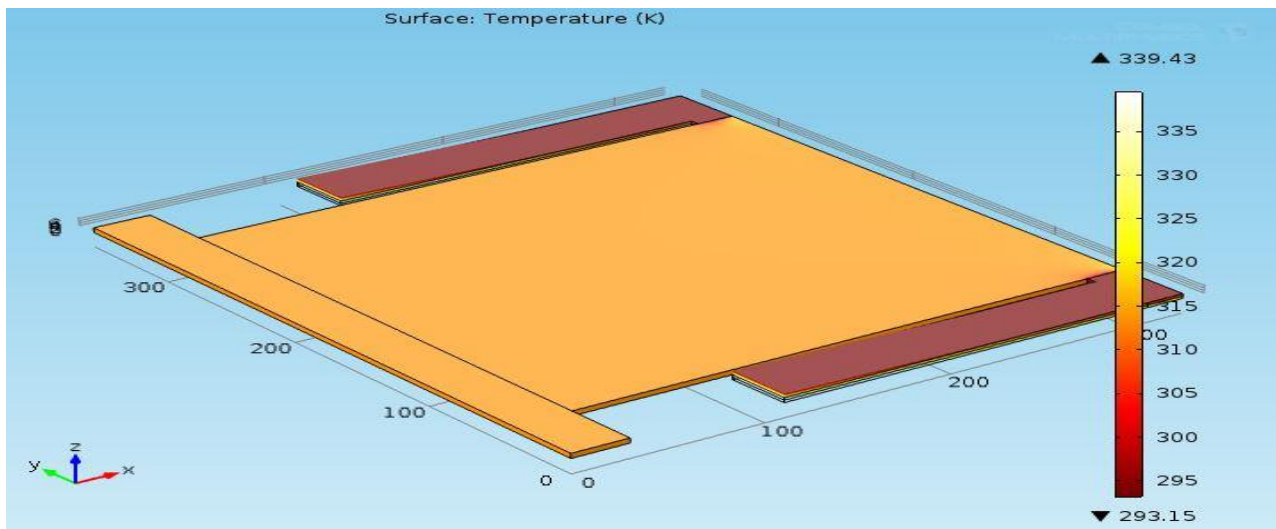


Figure 3.4.18: Temperature Analysis, rise in temperature from 295K to 337K

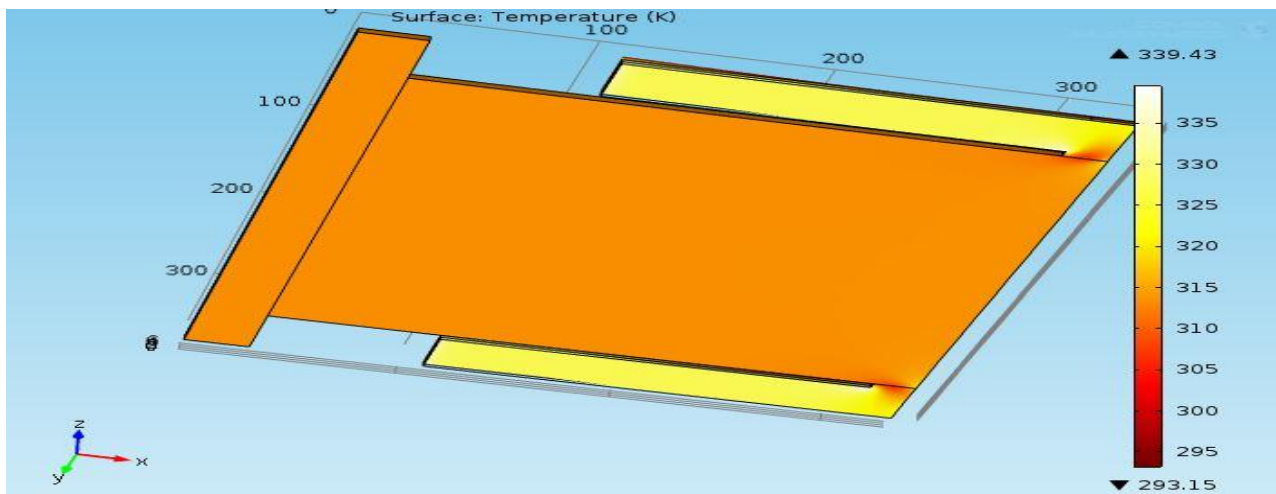


Figure 3.4.19: Temperature Analysis, Back view of the device

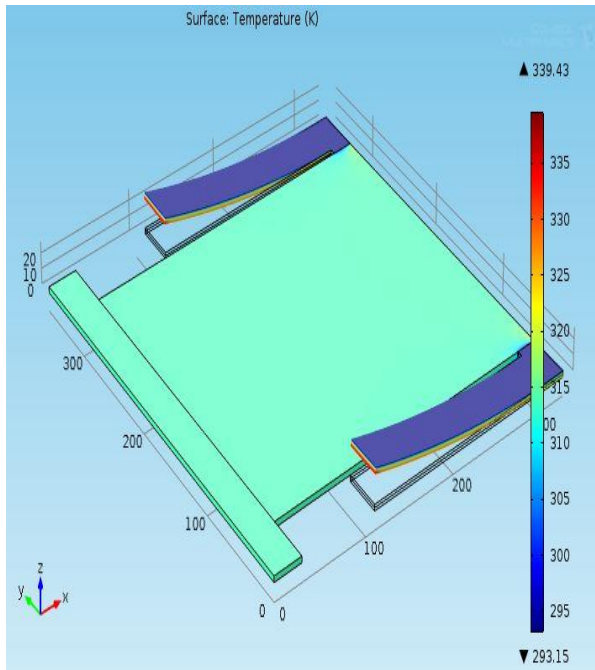


Figure 3.4.20: Deflection with rise of Temp

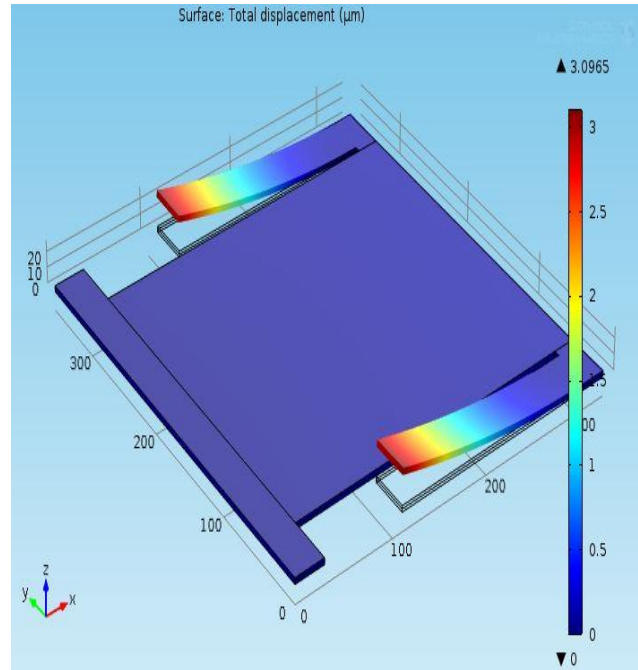


Figure 3.4.21: Corresponding displacement

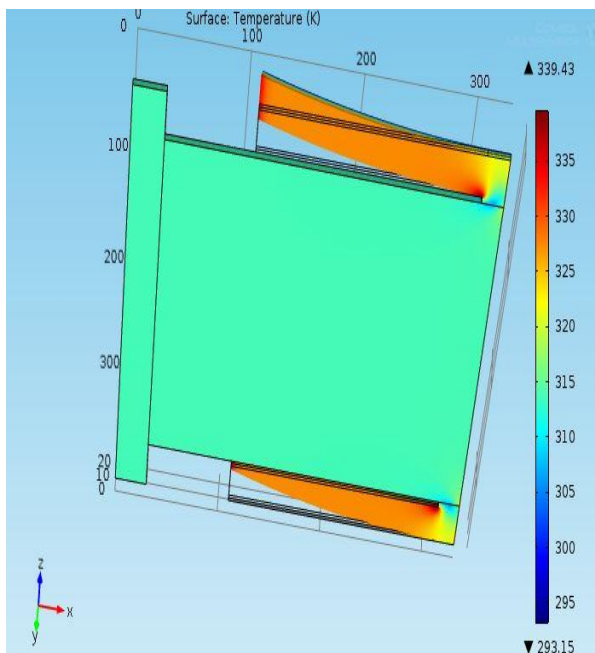


Figure 3.4.22: Back view of device

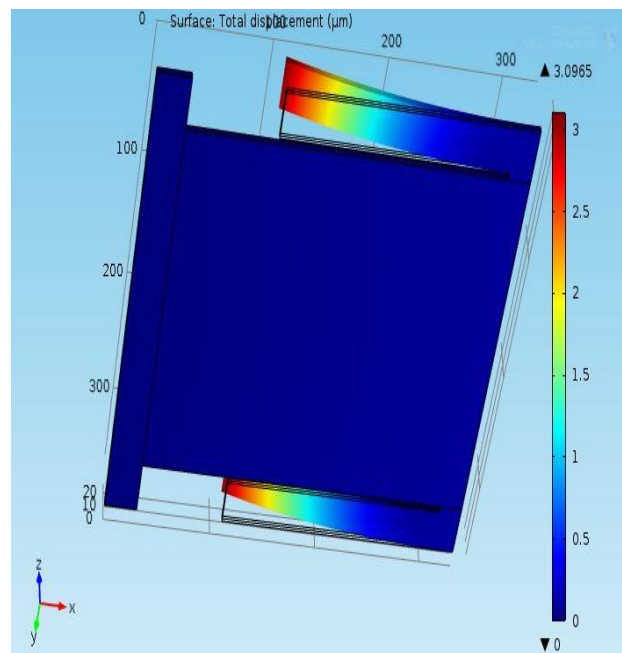


Figure 3.4.23: Back view displacement of bimorph

The results shown above correspond to the rise in temperature from 295K to the usual increase of the temperature of structures and the corresponding deflection/ displacement of bimorph as the temperature increases. The bimorph portion deflects towards the upper side with a total displacement of 0 μ m to 3 μ m with an increase of temperature from 295K to 337K respectively.

The voltage Vs displacement graph of the bimorph showing the voltage values for the displacement rising from 0v to 1v compared to 0 μ m to 3 μ m along with the corresponding field voltage is represented in the figures 3.4.24 and 3.4.25 respectively.

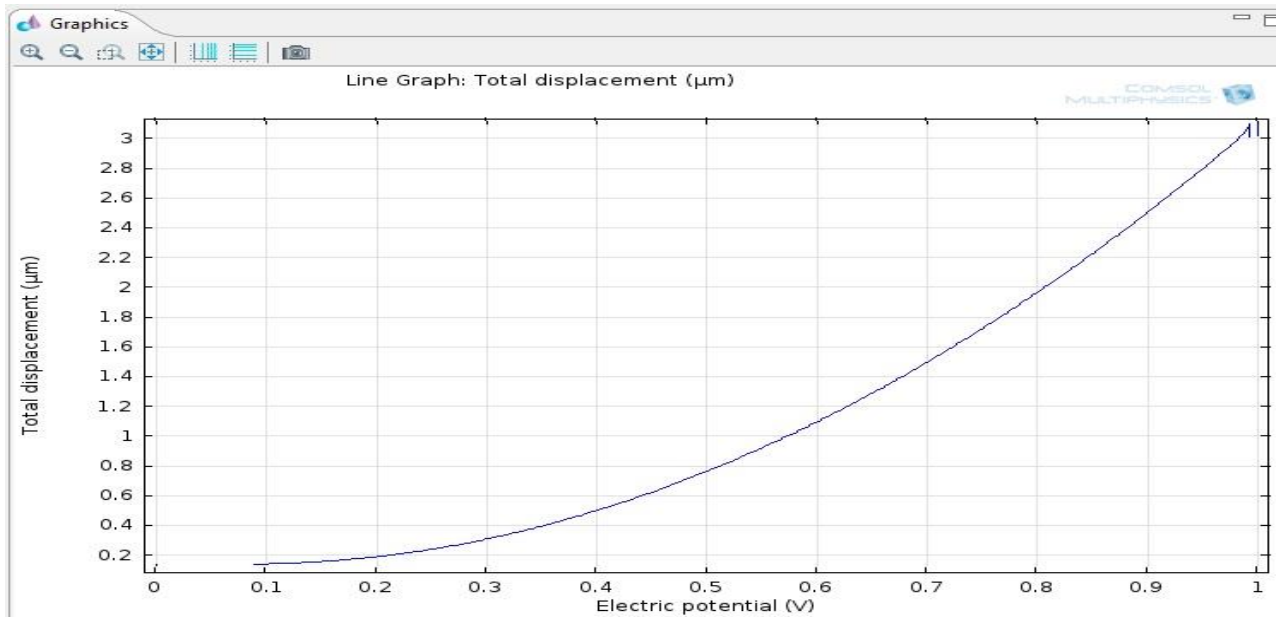


Figure 3.4.24: Voltage vs Displacement graph

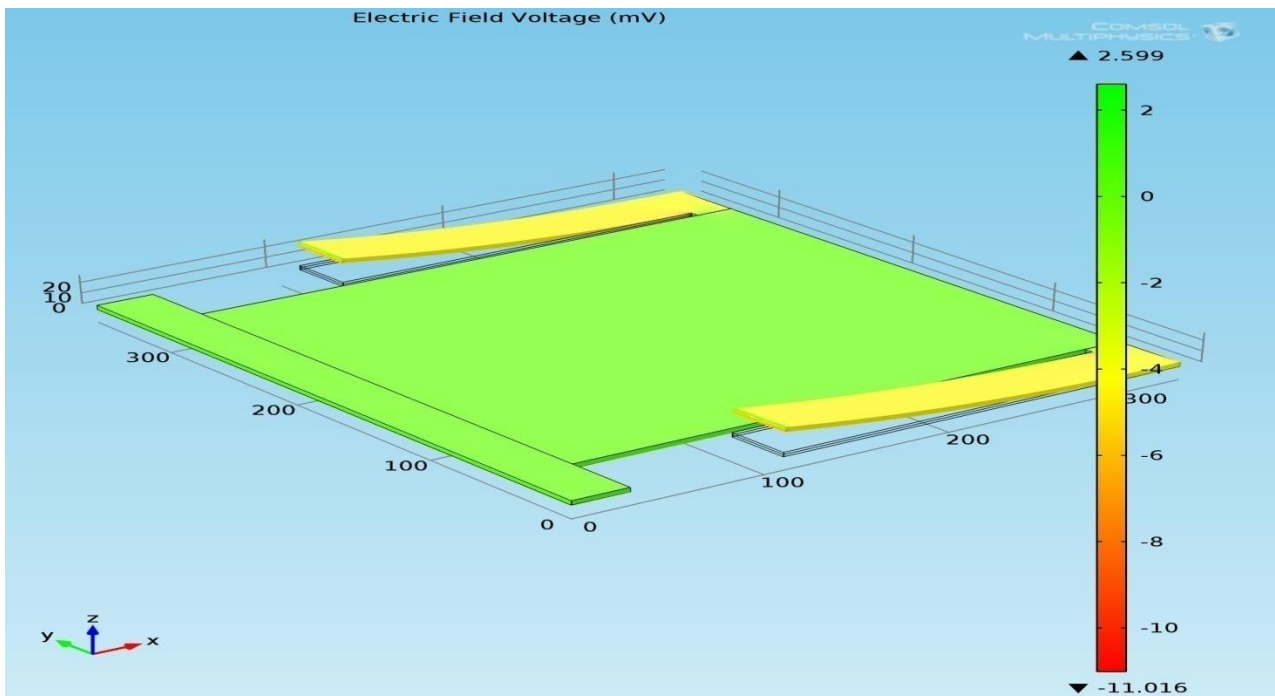


Figure 3.4.25: Corresponding field voltage

Next the displacement of main mass is shown in figure 3.4.26. The graph shows the displacement of main mass as it displaces with respect to the temperature increase.

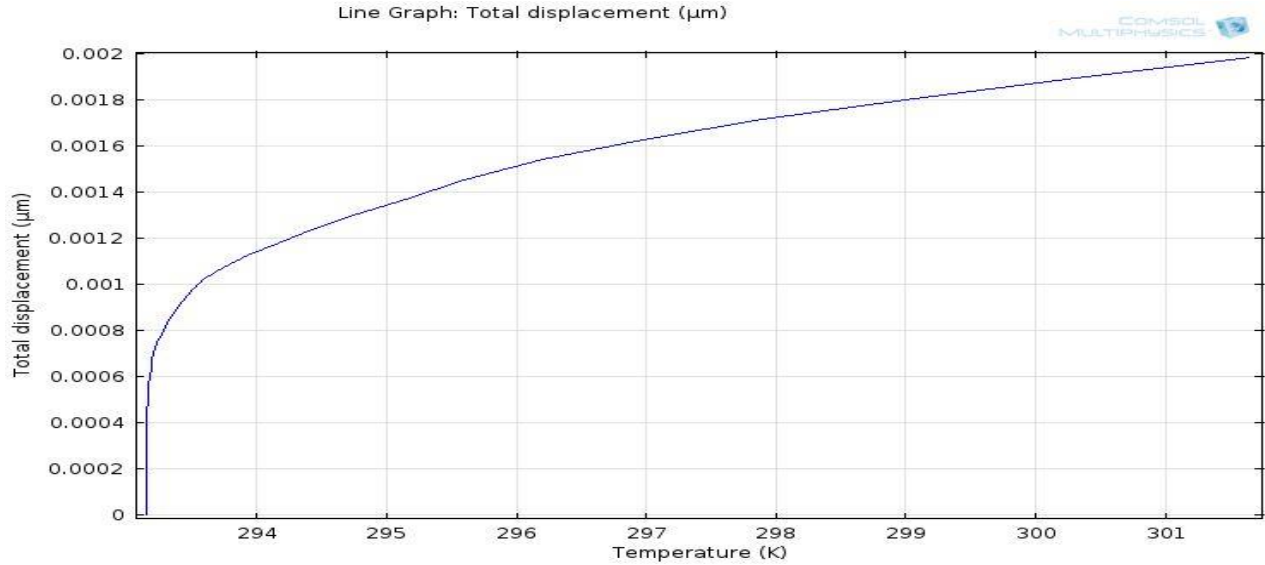


Figure 3.4.26: Graph representing displacement of main mass with temperature rise

The displacement of main mass is hence negligible in comparison with the displacement of bimorph.

3.4.5 Concrete Envelope Device Closure

The packaging of the device is not the scope of this study however to see the effect of concrete temperature on the device voltage output it is enclosed in the concrete envelope as shown in figure 3.4.27. The temperature of concrete is increased from 295K to 337K

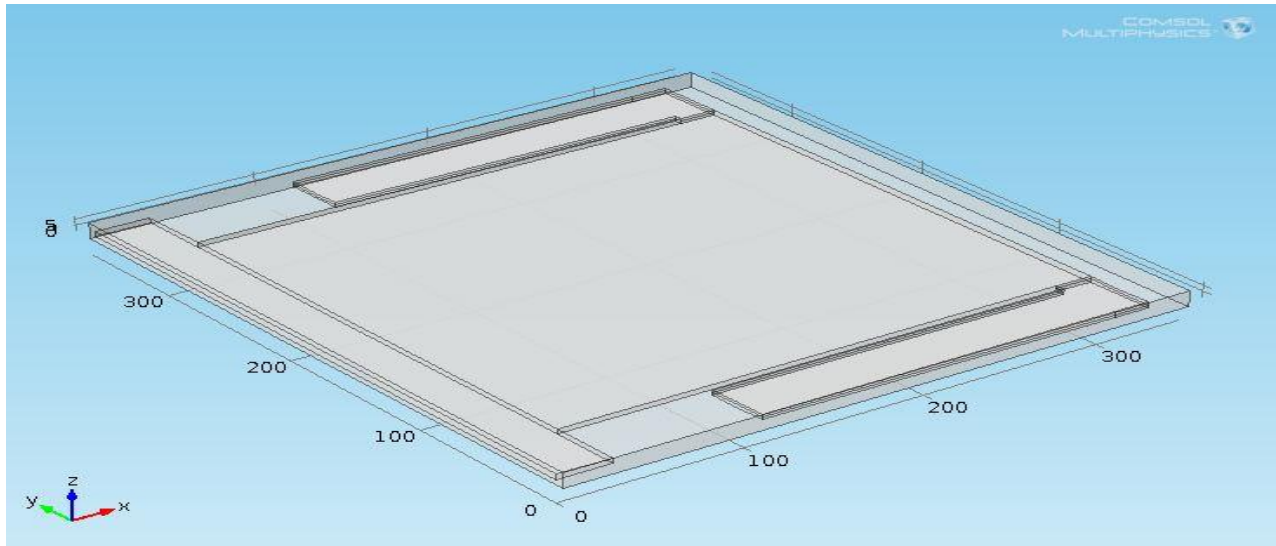


Figure 3.4.27: Concrete envelope around device

The size of the envelope is $340\mu\text{m} \times 375\mu\text{m}$ with a thickness of $12\mu\text{m}$. Envelope is designed to analyze the temperature effect on the device. The simulation results are shown in figure 3.4.28

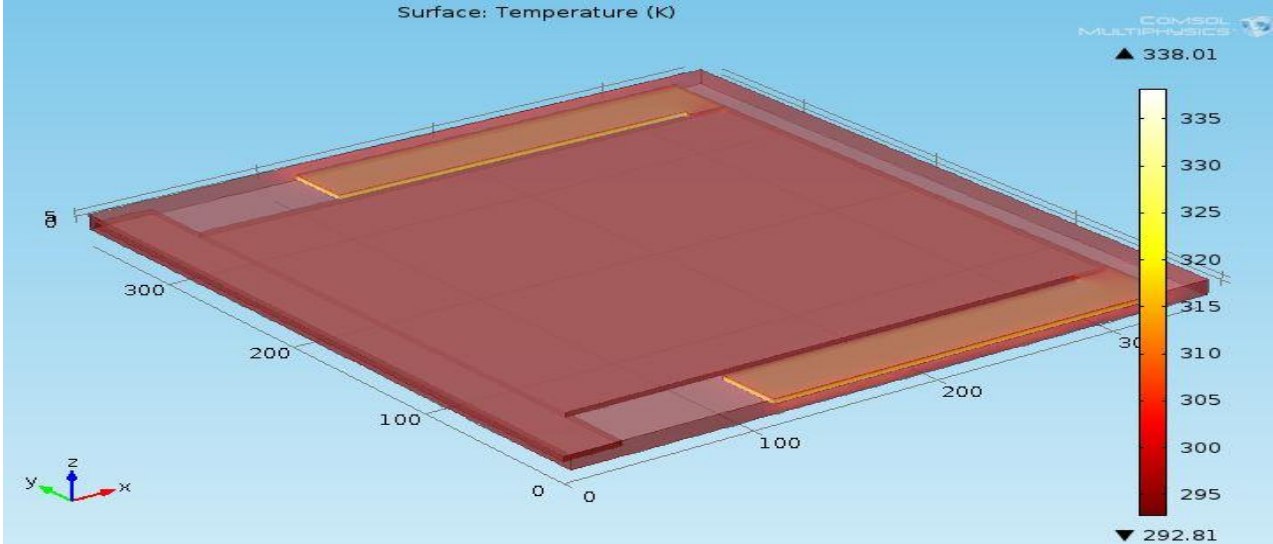


Figure 3.4.28: Effect of increasing temperature

The effect of temperature increase on the voltage output of the device can be seen in the figure 3.4.29.

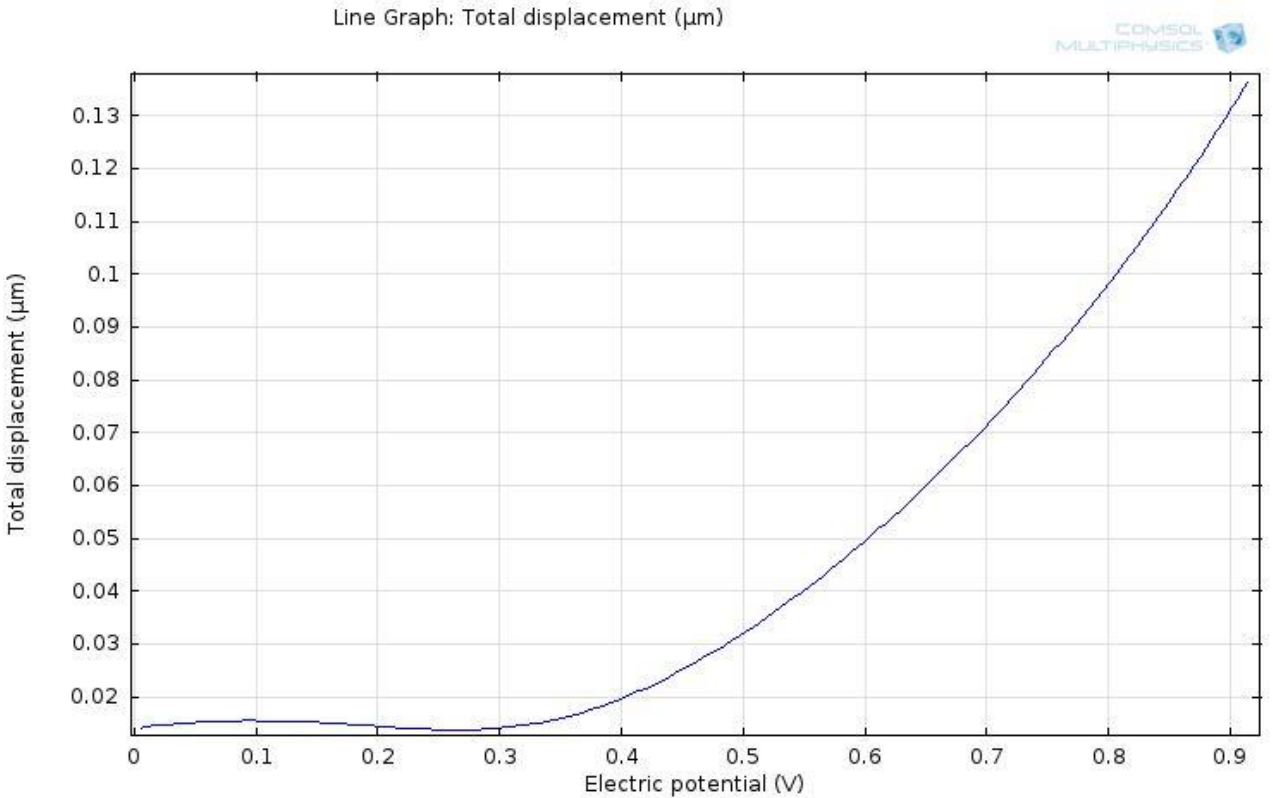


Figure 3.4.29: Effect on voltage due to rise in temperature corresponding to displacement

CHAPTER 4: RESULTS, DISCUSSION AND CONCLUSION

This chapter focuses on the discussion on mathematical and simulation results presented in chapter 2 and chapter 3 in detail. The primary focus of the chapter is to discuss the flaws of the early designs (first 3 designs) and merits of the final design.

4.1 Energy Harvester Design 1(electrostatic)

Figures 3.1.2, 3.1.3 and 3.1.4 show the simulation results of design 1. It can be clearly seen that the displacement in figure 3.1.2 is too less compared to the boundary load applied at boundary of the energy harvester; further figure 3.1.3 shows the stress on the device which shows that the device is unable to withstand the load and the device exhibits irregular behavior. Figure 3.1.4 shows that the serpentine springs have very low stiffness not able to hold the device. Due to the spring stiffness the design was changed and stiffness was increased.

4.2 Capacitive Energy Harvester Design (Design 2)

Design 1 was modified into capacitive energy harvester by introducing comb fingers, anchor and increasing the serpentine spring stiffness. The simulation results under the section 3.2.1 reveal that the displacement of main mass is within the permissible limits where as the serpentine springs stiffness is again too low to hold the device and act as bimorph, moreover modal analysis exposes the design flaws of comb fingers. The graph shown in the section shows the capacitance results which is too low and not in the acceptable values of using the device as energy harvester. The joule heating analysis of the device also reveals the serpentine springs deflect/ bend in such a way that the comb fingers get damaged by getting in touch with the device anchor. The design was further investigated by increasing the comb fingers increasing the number to 60 comb fingers with a distance of $1\mu\text{m}$ which become complex to fabricate by the available fabrication techniques due to which design was not further investigated and the focus was shifted towards piezoelectric energy harvesters due to the advantages of piezoelectric harvester upon other types.

4.3 Bimorph Piezoelectric Energy Harvester (Design 3)

The design is shown in figure 3.3. The piezoelectric energy scavenger in the design is a bimorph i.e. the idea is to harvest the energy from the device along with using the same as temperature

sensor. The five cantilevers are used which harvest the energy once they are loaded by a mechanical force under the principle of piezoelectricity. The simulation results shown in figure 3.3.1, 3.3.2 and 3.3.3 under the section 3.3.1 correspond to the bimorph harvester under discussion. It can be seen in the figure that the displacement is acceptable to some extent but natural frequency and voltage at the same are among unacceptable results as the frequency reaches a very high values with a very low output voltage, moreover, there are five cantilever beams which mean that the design would require as many means to measure the temperature and harvest the proper energy from these making the technique complex and cumbersome. Due to the reasons mentioned above the design is not further investigated.

4.4 Piezoelectric Energy Harvester with Temperature Sensor (Bimorph)

The piezoelectric energy harvester with temperature measuring bimorph has already been explained in the previous chapters. The addition in the device is the concept of temperature measurement through bimorph which makes the device different from other energy scavenger devices. This additional feature as already explained previously is helpful in measuring the temperature of the structure in which it is to be embedded so directly giving the information about the condition of the structure.

Firstly the device is tested for different thicknesses so as to get the best results. The results are simulated for thicknesses $8\mu\text{m}$, $6\mu\text{m}$ and $4\mu\text{m}$. Results in figures 3.4.1, 3.4.2, 3.4.3 and 3.4.4 correspond to the displacement and voltage simulation results for these thicknesses respectively. It is clearly seen that the lowest displacement and voltage results are shown when the thickness is $8\mu\text{m}$ i.e. $2.68 \times 10^{-4}\mu\text{m}$ for displacement and $2.64 \times 10^{-4} \text{V}$ for the voltage correspond to very low results. As the thickness is decreased the results are better as for $6\mu\text{m}$ thickness the results are effectively increased to $4.7739 \times 10^{-4}\mu\text{m}$ and $1.16 \times 10^{-4} \text{V}$ whereas for the thickness of $4\mu\text{m}$ the results are $4.3 \times 10^{-3}\mu\text{m}$ and 4.958mV . The comparison of results shows that $4\mu\text{m}$ is the ideal choice for further investigation of the device. The results of displacement are negligible for thicknesses $8\mu\text{m}$ and $6\mu\text{m}$ compared to that with $4\mu\text{m}$ and similarly for the voltage too where the difference is quite significant. The reason is the mobilization of ions is relatively more and rapid in the device having thin piezoelectric layer than devices with thick layers, moreover the flexibility of the device is important phenomenon too. So as we move towards less thickness of the piezoelectric materials the results are better taking into account the ability to withstand the stresses under the

designed conditions. Figure 4.1 shows the graph of the theoretical calculations of displacement done in chapter 2 along with the simulated results of the displacement for the thickness of 4 μm where displacement is taken along the y-axis and length of the device along the x-axis.

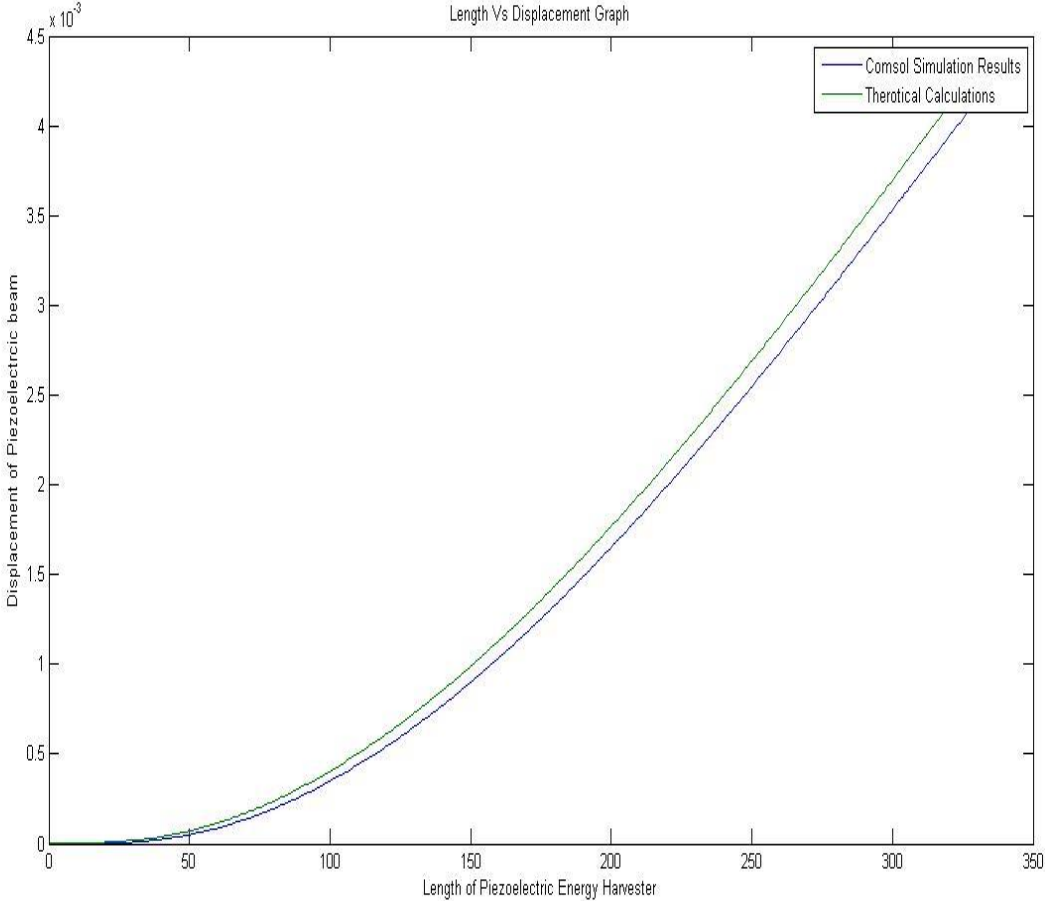


Figure 4.1: Graph showing comparison of Theoretical calculations and simulation results for displacement of the device

Further the device is subjected to frequency analysis and the simulations results in figure 3.4.5 and figure 3.4.6 shows the natural frequency of 17761 Hz with a displacement of 0.2738 μm and a voltage of 2.0182 V further showing the effectiveness of the designed harvester. The device is subjected to modal analysis which also shows quite satisfactory results with the maximum displacement and voltage being simulated at the natural frequency or first modal frequency, as the resonance frequency is the one at which the maximum displacement and voltage of the device appears. Harmonic sweep is applied to see the behavior of the device at different frequencies under the dynamic conditions. A harmonic sweep is applied and results are presented in figures 3.4.13

through 3.4.17 for frequency of 500Hz, 5500Hz, 13500Hz and 17000Hz. The results show the maximum voltage is simulated at frequency of 17500Hz already presented in the graph in figure 3.4.17. The device is subjected to the harmonic sweep in the range of 500Hz and 17500Hz, the results shown in chapter 3 are the selected ones to give an idea of the output of the device at different frequencies and it is seen during the simulations that the best results appeared near the natural frequency of the device. The results are tabulated below in table 4.1.

S. No.	Frequency	Displacement	Voltage
1.	500 Hz	$4.3032 \times 10^{-3} \mu\text{m}$	$9.2875 \times 10^{-3} \text{ V}$
2.	5500 Hz	$4.7226 \times 10^{-3} \mu\text{m}$	0.0216 V
3.	13000 Hz	$9.6982 \times 10^{-3} \mu\text{m}$	0.039 V
4.	17500 Hz	0.134 μm	0.0673 V

Table 4.1: Harmonic Sweep Results

The device is then simulated for temperature analysis results as presented in section 3.4.4.1. The concept of bimorph is used as the bimorph deflects/ bends in the direction of the material with low coefficient of expansion among the two. The results are presented in figure 3.4.18 clearly show that when temperature is raised from 295K to 339K the bimorph achieves a displacement of $3.0965 \mu\text{m}$ as presented in figure 3.4.21.

The graph shown in figure 3.4.24 shows the rise in displacement and voltage. For 295K the displacement is $0 \mu\text{m}$ and the voltage is also 0V whereas at 339K the displacement is $3.0965 \mu\text{m}$ recording a voltage of 1V. Similarly graph can be related to other displacements i.e. by measuring the voltage and displacement temperature can be easily estimated hence the health of the structure can be inspected by observing these parameters. The displacement of main mass is presented in figure 3.4.26, as can be seen that the displacement of merely $0.002 \mu\text{m}$ is achieved (main mass displacement) at the temperature of 304K whereas at the same temperature the displacement of bimorph is approximately $0.5 \mu\text{m}$, hence the displacement of main mass is neglected. A concrete envelope is developed around the device so as to check the results of the device in such environment. Here too the temperature is increased and the figures 3.4.27 through 3.4.39 show the results that the displacement of main mass is pretty much less as compared to the bimorph, moreover the voltage results are a bit different than the open environment as at low displacement the voltage reaches 1V.

4.5 Conclusion

Cantilevered based single layer Piezoelectric Energy Harvester with integrated temperature sensor shows quite commendable results as displacement simulation results are verified through theoretical calculations also. The interesting feature is measurement of temperature of the structure through the same device. There exists a lot of potential in this design as the concept of measuring temperature along with the scavenging energy which is the premier objective of the thesis is achieved successfully. The voltage output of 2.01 V could be used for the portable electronics embedded in the structure plus it can also give the insight of the structure by not only measuring the temperature but also the frequency and vibrations of the structure and can lead to the analysis of the structure to determine its various characteristics to access the life time and condition of the structure in which the device is embedded. The thickness of the device is selected through carefully simulating the device for various piezoelectric thicknesses and selecting the one with the best output results and strength bearing capacity. The displacement results match closely with the results and natural frequency of the device depicts a wide range of operation in which the device can be operated showing admirable results. The proposed method to measure the temperature change is by using optical techniques that have been developed for MEMS. Further the voltage change analysis of the temperature sensor can also be observed using the same optical techniques.

Chapter 5: Fabrication Technique and Future work

Micro electro mechanical system (MEMS) fabrication is a greatly energizing enterprise because of the modified way of procedure advances and the differences of handling capacities. MEMS manufacture utilizes huge numbers of the same strategies that are utilized as a part of the incorporated circuit space, for example, bulk micromachining, surface micromachining, oxidation, dispersion, particle implantation, LPCVD, sputtering, ion etching and so on, and consolidates these capacities with very specific micromachining procedures [33].

5.1 Sputtering

Sputtering is a procedure in which atoms are shot out from a solid material because energetic particles hit the target as they are bombarded on to it, a solid object substance deposition takes place under vacuum on a solid. It just happens when the active vitality of the approaching particles is much higher than customary thermal energies of the particles ($\gg 1$ eV). This procedure can lead, amid delayed particle or plasma barrage of a material, to noteworthy disintegration of materials. It is usually used for deposition of thin films, analytical techniques, deposition and etching. Among the basic sputtering techniques are magnetron technique used for deposition, reactive sputter deposition, diode sputter deposition technique, ion assisted deposition and radio frequency (RF) sputter deposition [34].

Sputtering is viewed as a physical, as opposed to compound, process in light of the fact that the material does not regularly experience any substance piece changes amid statement. Amid sputtering, episode particles, more often than not particles, strike the surface of the objective material. On the off chance that the occurrence iotas have adequate vitality they will bring about the discharge of target molecules in the wake of crashing into the surface. Most sputter frameworks supply the occurrence particles as a plasma and draw in the particles with voltage connected to the objective which is situated at the cathode. The substrate and load are grounded, to guarantee safe operation. Particles are catapulted from the surface of the objective and kept all through the vacuum chamber in a line of site bearing.

The progressions in the sputter testimony procedure are clearing of the vacuum chamber, refill with working gas, touch off the plasma, clean the objective, lastly store material. Sputtering must happen in ultra high vacuum conditions to guarantee that the mean free way of sputtered molecules is adequate to head out from the objective to the substrate. The working gas, ordinarily Ar or Ne, is

ionized to make the plasma. Higher sputter yield is acknowledged with higher mass gasses, so Ar is the most generally utilized working gas. The applying so as to work gas is ionized a vast voltage to it. A DC or RF power supply applies the voltage to the cathode, contingent upon the material to be kept. A wide mixed bag of materials can be sputtered, including metals, separators and semiconductors. Ordinarily DC sputtering is utilized to store metals and RF (13.56 MHz) sputtering is utilized to store covers.

An alternate system of physical sputtering is warmth spike sputtering. This may happen when the strong is sufficiently thick, and afterward the approaching particle sufficiently overwhelming, that the impacts happen near one another. At that point the parallel impact estimate is no more legitimate, yet rather the collisional procedure ought to be comprehended as a numerous body process. The thick crashes impel a warmth spike (additionally called warm spike), which basically dissolves the gem provincially. On the off chance that the liquid zone is sufficiently close to a surface, huge quantities of particles may sputter because of stream of fluid to the surface and/or micro explosions. Heat spike sputtering is most vital for substantial particles (say Xe or Au or group particles) with energies in the keV–MeV extent barraging thick yet delicate metals with a low softening point (Ag, Au, Pb, and so forth.). The warmth spike sputtering regularly increments nonlinearly with vitality, and can for little bunch particles lead to emotional sputtering yields per group of the request of 10,000 [35] [36] [37].

5.2 Electron Beam (e-beam) Evaporation

Thermal evaporation corresponds closely with the electron beam evaporation technique which is ideal for the lift off structures. A source material is warmed over its bubbling/sublimation temperature and vanished to frame a film on the surfaces that is stroke by the dissipated particles. This dissipation system has recently like warm vanishing a pore capacity to cover steps which additionally makes this strategy perfect for lift-off procedure. With the source material set in the cauldron a fiber beneath the pot is warmed. By applying a substantial voltage, electrons are drawn from the fiber and engaged as a pillar on the source material by a few twisting magnets. The bar is cleared over the surface of the source material to warmth the greater part of the material. An observable point of preference of e-shaft vanishing over warm dissipation is the likelihood to include a bigger measure of vitality into the source material. This yields a higher thickness film with an expanded attachment to the substrate. Since the electron shaft just warms the source material and not the whole pot, a lower level of sully from the cauldron will be available than

on account of warm dissipation. By utilizing a various pot E-beam firing mechanism, a few unique materials can be saved without breaking the vacuum [38] [39] [40].

5.3 Fabrication Steps

The detail of fabrication steps is presented in the figures below. Step by step process of fabrication to be followed as depicted. Sputtering deposition followed by e-beam evaporation techniques are proposed for the fabrication of the device.

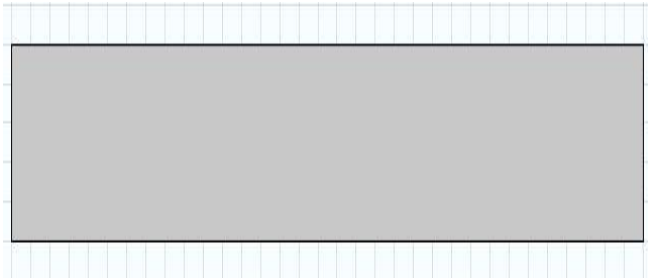


Figure 5.1: Silicon Deposition

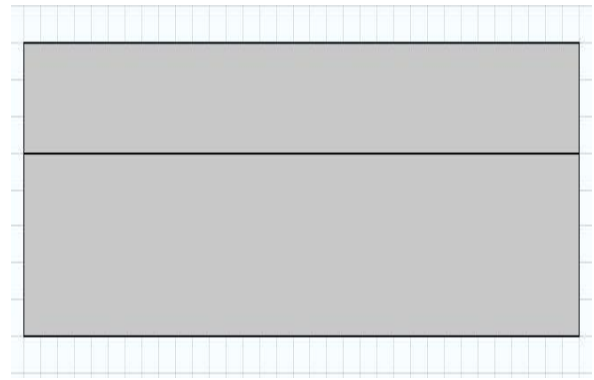


Figure 5.2: PZT layer deposition

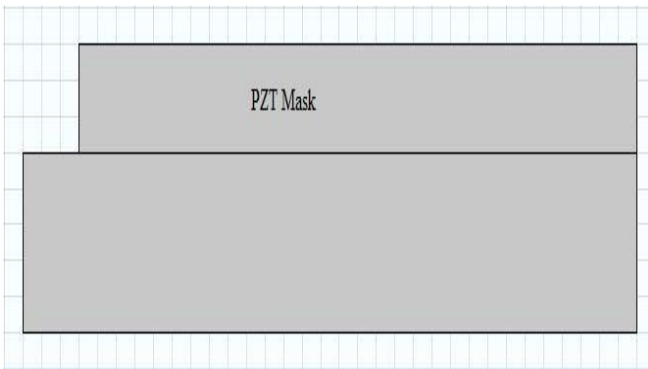


Figure 5.3a: Etching of PZT layer

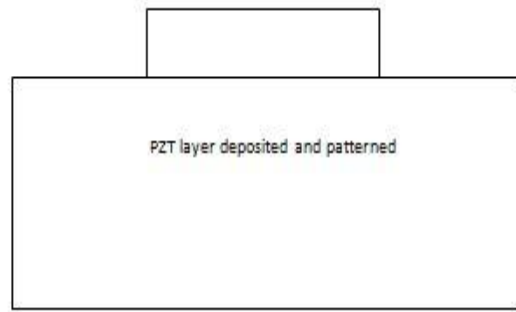


Figure 5.3b: A view from Anchor side

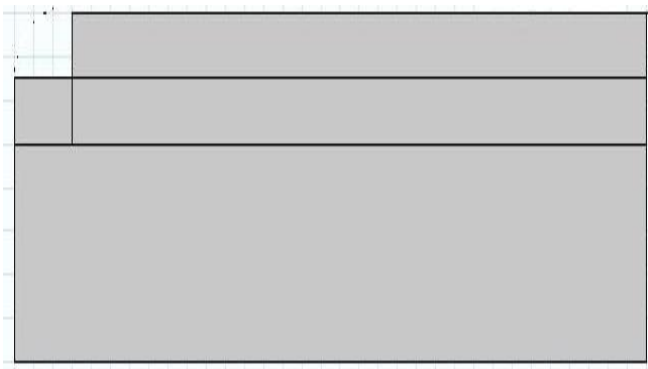


Figure 5.4: Deposition of Ag Layer

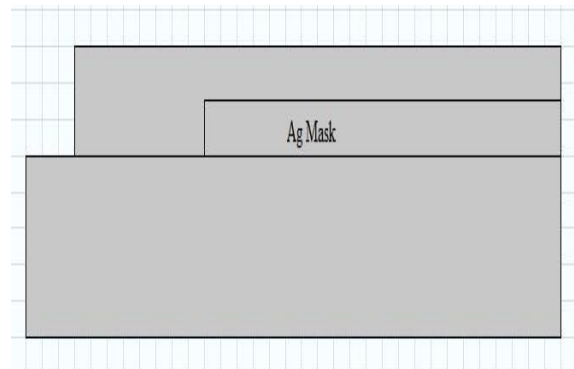


Figure 5.5a: Patterning of Ag layer

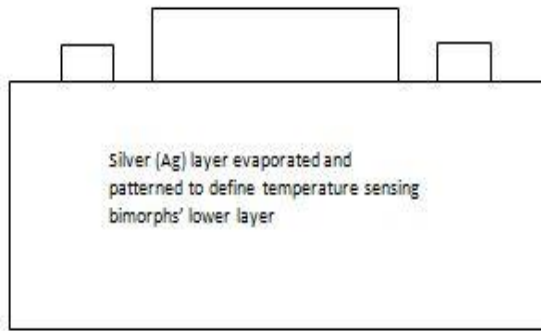


Figure 5.5b: View from anchor side

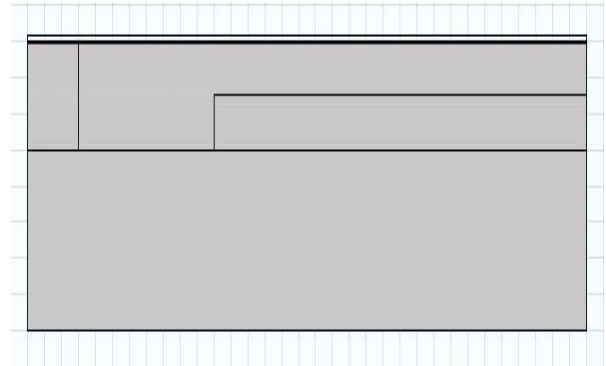


Figure 5.6: Al Layer Deposition

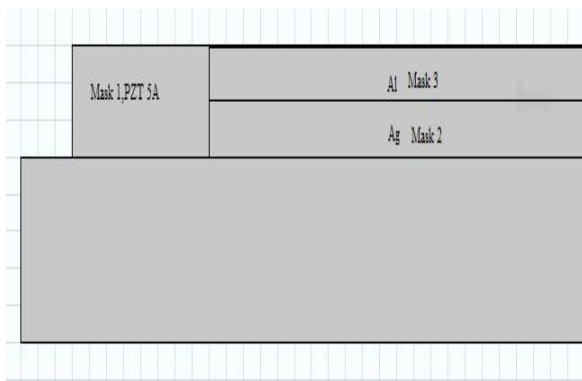


Figure 5.7a: Patterning of Al layer

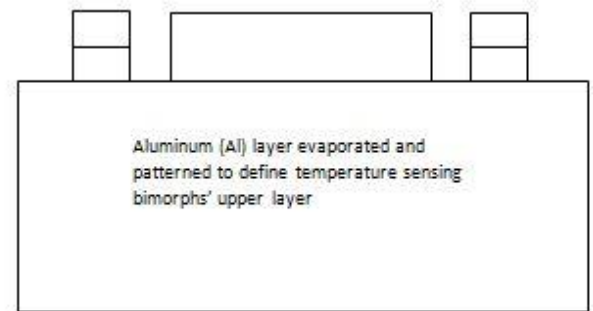


Figure 5.7b: View from Anchor side

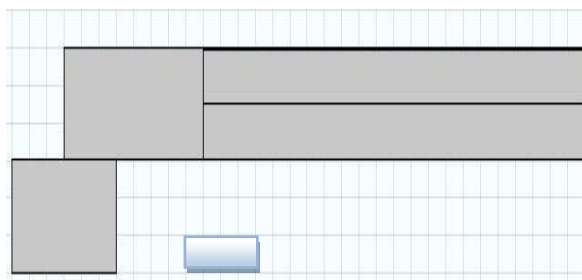


Figure 5.8a: Back side Etching to free the device

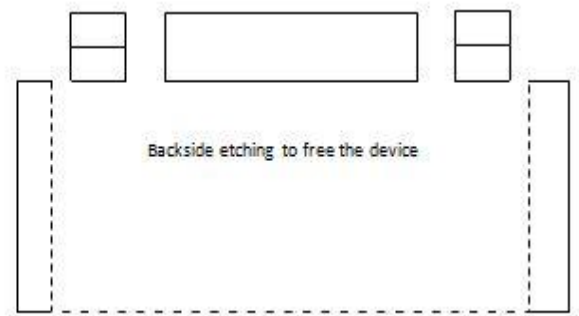


Figure 5.8b: View from anchor side

The above figures (figures 5.1 through figures 5.8) represents step by step scheme of fabrication for the device. Firstly silicon layer is to be deposited upon which PZT is to be deposited using sputtering deposition technique, followed by etching of PZT layer hence depositing the mask of PZT. Next Ag layer and deposition is to be deposited, the first of the bimorph layer followed by its etching and deposition of Al layer and its mask, the final etching of the layer followed by e-beam evaporation from the back side for lift off structures completes the fabrication process as can be seen in figure 5.8.

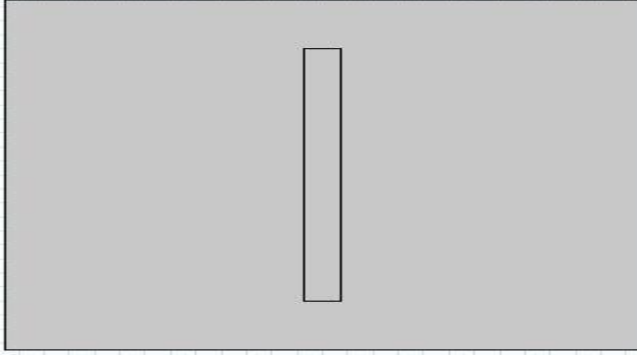


Figure 5.9: Anchor mask, Top view

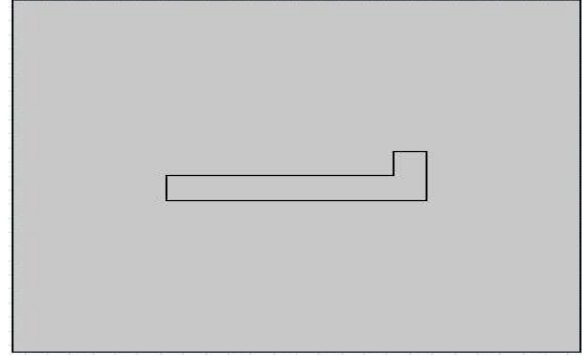


Figure 5.10: Bimorph mask, Top view

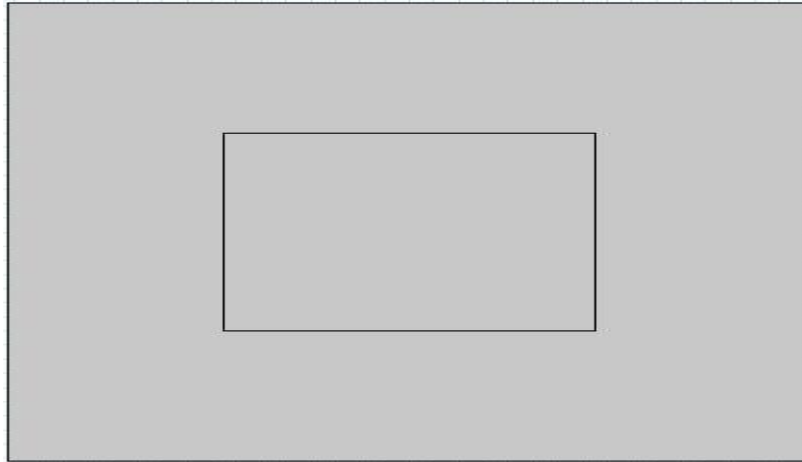


Figure 5.11: PZT mask, Top view

Figure 5.09, 5.10 and 5.11 show the top view of masks of anchor, bimorph and PZT respectively.

5.4 Future Work

Cantilevered based single layer piezoelectric energy harvester with integrated temperature sensor design can be further modified by implementing a permanent method to measure the temperature at the spot i.e. from the device/ bimorph itself. A MEMS wheatstone bridge can be implemented over the bimorph to directly access the temperature change by using variable resistive method. The technique will work as one of the resistance values of resistor that is variable will be changed as the result of the temperature change and hence helpful in directly measuring the temperature instead of using optical techniques which will make the system less cumbersome and economical too. Data acquisition system will have to be implemented for making the device fully autonomous. Moreover, piezoelectric system may be damped for making it useable for low frequency applications. Damping the system will help to achieve low frequencies as the natural frequency will be damped. Sensitivity of the device can be increased by applying slot defect mechanism in

the main mass, as by developing small holes the mass will become more sensitive to the input changes/ vibrations in the structure. Furthermore, the piezoelectric layer can also be made a bimorph which will help in harvesting more energy out of the device. Device design further needs to be modeled for the dynamic response and parallel redesign to withstand the changes in the modeling of the device.

REFERENCES

- [1] ACI Committee Report “ACI 228.2R-98” “Non-Destructive Test Methods for Evaluation of Concrete in structures”
- [2] ACI Committee Report “ACI 201.1R” Guide for Making a Condition Survey of Concrete in Service
- [3] Alexander, A. M., and Thornton, H. T., Jr. (1989). “Ultrasonic Pitch-Catch and Pulse-Echo Measurements in Concrete,” *Nondestructive Testing of Concrete*, H. S. Lew, ed., ACI SP-112, American Concrete Institute, Farmington Hills, Mich., Mar., pp. 21-40.
- [4] Grosse, C.U.: Monitoring of large structures using acoustic emission techniques. Symposium "Niet-destructief onderzoek in de bouwsector", Proceedings, Antwerpen, 23.10.2003, pp 15-24
- [5] Doherty, L., Warneke, B.A., Boser, B., Pister, K.S.J.: Energy and Performance Considerations for Smart Dust. International Journal of Parallel and Distributed Sensor Networks, Dec 2001
- [6] Baas, B.M.: A low power, high-performance, 1024-point FFT processor. IEEE J. Solid-State Circuits, 34(3), 1999, p. 380-387
- [7] Prine, D.W. (1995) “Problems Associated with Nondestructive Evaluation of Bridges,” *Proceedings: Nondestructive Evaluation of Aging Infrastructure*, SPIE, Oakland, CA, 46-53.
- [8] Basheer, P. A. M.; Montgomery, F. R.; and Long, A. E. (1992). “In Situ Assessment of Durability of Concrete Motorway Bridges,” *Durability of Concrete: G.M. Idorn International Symposium*, J. Holm and M. Geiker, eds., ACI SP-131, American Concrete Institute, Farmington Hills, Mich., pp. 305-319.
- [9] ASTM Standards “ASTM C 1202 Test Method for Electrical Indication of Concrete’s Ability to Resist Chloride Ion Penetration”
- [10] ASTM Standards “ASTM C 803 Test Method for Penetration Resistance of Hardened Concrete”
- [11] British Standards “BS 1881 Part 5: Methods of Testing Concrete for Other Than Strength”
- [12] Bungey, J. H., and Millard, S. G. (1993). “Radar Inspection of Structures,” *Proceedings, Institute of Civil Engineers, Structures and Buildings Journal (London)*, V. 99, May, pp. 173-186.
- [13] Davis, A. G., and Hertlein, B. H. (1997). “Evaluation of the Integrity of Some Large Concrete Foundations Using NDT,” ACI SP-168, *Innovations in Nondestructive Testing of Concrete*, S. Pessiki and L. Olson, eds., pp.333-356.
- [14] Rodríguez, P.; Ramírez, E.; and González, J. A. “Methods for Studying Corrosion in Reinforced Concrete,” *Magazine of Concrete Research*, V. 46, No. 167, June, pp. 81-90.
- [15] Scott W. Doebling, Charles R. Farrar, and Michael B. Prime “A summary review of vibration-based damage identification methods”
- [16] Poulin, G.; Sarraute, E.; Costa, F. Generation of electrical energy for portable devices: Comparative study of an electromagnetic and a piezoelectric system. *Sens. Actuator A Phys.* **2004**, *116*, 461–471.

- [17] Rabaey, J. M., Ammer, M. J., da Silva, J. L., Patel, D. And Roundy, S., "Picoradio Supports Ad Hoc Ultra-Low Power Wireless Networking," *Computer*, 33, pp. 42-48(2000)
- [18] Henry A. Sodano, Daniel J. Inman and Gyuhae Park , "A Review of Power Harvesting from Vibration using Piezoelectric Materials"
- [19] B. S. Lee, S. C. Lin and W. J. Wu, "Fabrication and Evaluation of a MEMS Piezoelectric Bimorph Generator for Vibration Energy Harvesting"
- [20] Elvin, N. G., Elvin, A. A. and Spector, M., "A Self-Powered Mechanical Strain Energy Sensor," *Smart Materials and Structures*, 10, pp. 293-299 (2001)
- [21] Roundy, S., Wright, P. K. and Rabaey, J., "A Study of Low Level Vibrations as a Power Source for Wireless Sensor Nodes," *Computer Communications*, 26, pp.1131-1144 (2003)
- [22] Renaud, M.; Karakaya, K.; Sterken, T.; Fiorini, P.; Van Hoof, C.; Puers, R. Fabrication, modeling and characterization of MEMS piezoelectric vibration harvester
- [23] Muralt, P.; Marzencki, M.; Belgacem, B.; Calame, F.; Basrour, S. Vibration energy harvesting with PZT micro device
- [24] Hua Yu, Jieli Zhou , Licheng Deng and Zhiyu Wen "A Vibration-Based MEMS Piezoelectric Energy Harvester and Power Conditioning Circuit"
- [25] Jeon, Y.B.; Sood, R.; Jeong, J.; Kim, S.-G. MEMS power generator with transverse mode thin film PZT. *Sens. Actuator A Phys.* **2005**, *122*, 16–22.
- [26] NASA/CR -1998-208708 "Properties of PZT-Based Piezoelectric Ceramics Between-150 and 250°C"
- [27] Venu GM Annamdas Madhav A Radhika Electromechanical impedance of piezoelectric transducers for monitoring metallic and non-metallic structures: A review of wired, wireless and energy-harvesting methods
- [28] Venu GM Annamdas and Madhav A Radhika "Electromechanical impedance of piezoelectric transducers for monitoring metallic and non-metallic structures: A review of wired, wireless and energy-harvesting methods "
- [29] Hwan-Sik Yoon , Se-hun Kim , Min-Hyuck Kim , Dongsoo Jung , Joo-Hyung Kim , Hyeon-Ju Kim and Ho-Saeng Lee , "Wireless piezoelectric strain sensing measurement using a frequency modulation technique"
- [30] Vinicius Augusto Dare de Almeida and Fabricio Guimarães Baptista , "An experimental assessment of pzt patches for impedance based SHM applications"
- [31] A. Brodgesell, B.G. Liptak and H. Eren, "Instrument Engineers handbook : Process and Measurement Analysis, Chapter 7, Vibration, Shock and Acceleration"
- [32] Géraldine Villain, Odile Abraham, Loïc LE Marrec and Lalaonirina Rakotomanana , "Determination of the bulk elastic moduli of various concrete by resonance frequency analysis of slabs submitted to degradations"
- [33] Rahman, A. and Raven, M.S., *Electrical Characteristics of RF-Sputtered Al₂O₃ MIM Structures*. *Thin Solid Films*, 1980. **71**(1): p. 7-13.
- [34] Rohde, S.L., *Sputter Deposition*, in *Surface Engineering*, 1994, ASM International
- [35] Seshan, K., ed. *Handbook of Thin-Film Deposition Processes and Techniques*. 2 ed. 2002, Noyes Publications: Norwich, NY

- [36] Stuart, R.V., *Vacuum Technology, Thin Films, and Sputtering: An Introduction*, 1983, New York: Academic Press.
- [37] Peterson, K.A., et al., *Novel Microsystem Applications with New Techniques in Low Temperature Co-Fired Ceramics*. *International Journal of Applied Ceramic Technology*, 2005. **2**(5): p. 345-363.
- [38] J. W. Dini 2. 3. 4. 5. 6. 7. 8. 9. Properties of Coatings: Comparison of Electroplated, Physical Vapor Deposited, Chemical Vapor Deposited and Plasma Sprayed Coatings”, *Materials and Manufacturing Processes* 12, (1997) 437-472
- [39] J. Singh Ion Beam Assisted, Electron Beam Physical Vapor Deposition, *Advanced Materials and Process* 11 (1996) 32
- [40] D. E. Wolfe Growth of TiN coatings by Reactive Ion Beam-Assisted, Electron Beam-Physical Vapor Deposition (RIBA, EB-PVD) and hard Coatings Evaluation MS Thesis, Penn state University, University Park, PA (1996).